

# Mass Spectrometry of Aerosols

David T. Suess and Kimberly A. Prather\*

Chemistry Department, University of California at Riverside, Riverside, California 92521

Received February 17, 1999 (Revised Manuscript Received July 16, 1999)

## Contents

I. Introduction	3007
II. Aerosol MS Overview	3009
A. Sample Introduction	3009
B. Aerosol Sizing Techniques	3010
C. Ionization Techniques	3010
D. Mass Spectrometers	3012
III. Off-line MS of Aerosols	3014
A. Laser Microprobe Mass Spectrometry (LAMMS)	3015
B. Secondary Ion Mass Spectrometry (SIMS)	3017
C. Inductively Coupled Plasma Mass Spectrometry (ICPMS)	3018
IV. On-Line MS of Aerosols	3018
A. Surface/Thermal Ionization Mass Spectrometry	3018
1. Davis (1973)	3018
2. Lassiter and Moen (1974)	3019
3. Myers and Fite–SIMP (1975)	3019
4. Stoffels–DIMS (1981)	3020
5. Allen and Gould–CAART (1981)	3020
6. Sinha and Friedlander–PAMS (1982)	3020
B. Laser Desorption/Ionization Mass Spectrometry	3021
1. Sinha (1984)	3021
2. Marijnissen (1988)	3022
3. Johnston and Murphy (1991)	3022
4. Johnston and Wexler–RSMS (1994)	3023
5. Murphy–PALMS (1994)	3024
6. Prather–ATOFMS (1994)	3026
7. Ramsey and Whitten (1994)	3028
8. Reents (1994)	3029
9. Russell and Murray (1994)	3029
10. Spengler, Kaufmann and Hinz–LAMPAS (1994)	3030
C. Newer Members to the Aerosol MS Field	3030
V. Discussion/Conclusions	3031
VI. Acknowledgments	3033
VIII. References	3033



David T. Suess was born in 1975. He received his undergraduate chemistry degree at the University of California, Davis in 1993. Currently, he is a third year graduate student at the University of California, Riverside working under Professor Kimberly Prather. His main interests consist of aerosol source characterization and field studies, which include ambient aerosol sampling from the Grand Canyon, AZ, and Bakersfield, La Jolla, and Riverside, CA.



Kimberly A. Prather was born (1962) in Santa Rosa, CA. She received her B.Sc. and Ph.D. degrees from the University of California, Davis (B.Sc. 1985, Ph.D. 1990). She started her academic career at the University of California, Riverside in 1992 where she is currently an Associate Professor of Chemistry. Her major research areas of interest include the development of instrumentation for the continuous analysis of aerosol particles. She is interested in applying new technology in field and lab studies in order to gain new insights into aerosol processes contributing to visibility reduction, regional and global pollution, and climate change.

## I. Introduction

Aerosols are becoming more widely recognized throughout the world due to their significant local, regional, and global impacts. Local impacts include vehicular emissions, wood burning fires, industrial processes, and other aerosol sources that can lead to urban air pollution and possible adverse health

effects. Regional problems comprise aerosol transport from areas of high emissions to relatively clean remote regions, while global warming and heterogeneous chemistry in both the troposphere and stratosphere influence the entire planet. By definition, aerosols are any particulate matter, solid or liquid, suspended in a gas. Examples include dust, fog,

smoke, or smog. Throughout this article, the term aerosol will be synonymous with particles. Over the years incredible amounts of research effort have been directed toward aerosols. Such areas include, but are not limited to, the study of human health effects, global warming, and heterogeneous chemistry.

Aerosols and their direct effect on human health are a major concern. Epidemiological studies have correlated elevated levels of particulate matter with decreased pulmonary function,<sup>1-3</sup> respiratory disease,<sup>1,4,5</sup> and increased mortality.<sup>6-9</sup> A number of recent studies have associated these correlations with particles less than  $2.5\ \mu\text{m}$ <sup>10</sup> as they are inhaled more deeply into the lungs where they may deposit and cause inflammation leading to lung injury.<sup>11</sup> These smaller particles are more dangerous and more reactive than larger particles because they have large surface-to-volume ratios. In addition they are commonly produced from gas-to-particle conversion or combustion processes which are known to produce mutagens such as polycyclic aromatic hydrocarbons (PAHs). Although still controversial,<sup>12,13</sup> from studies such as these most agree that there is a correlation between health effects and atmospheric particle concentration. Consequently, the United States Environmental Protection Agency (USEPA) has been required recently to add new standards<sup>12</sup> on fine particulate matter less than or equal to  $2.5\ \mu\text{m}$  ( $\text{PM}_{2.5}$ ).

Global warming has been a developing controversy, as early atmospheric models tend to overestimate global temperature increases due to greenhouse gas emissions.<sup>14</sup> Greenhouse gases, such as  $\text{CO}_2$ ,  $\text{NO}$ , and  $\text{CH}_4$ , absorb the sun's radiation, which should lead to an increase in the mean global surface temperature. Early models, based mainly on greenhouse gas emissions, predict nearly twice the observed increase in global temperature. To explain the smaller temperature increase, aerosols are now taken into consideration. It is proposed that particles less than approximately  $1\ \mu\text{m}$  have a direct effect on lowering global surface temperatures as they most efficiently scatter the sun's radiation. They also act as cloud condensation nuclei allowing for more cloud formation and a consequent increase in the earth's albedo. Consequently, when aerosol contributions along with other environmental considerations are included in more modern atmospheric models, much better agreement on global temperature increases are found.<sup>14-17</sup>

Aerosols and their participation in atmospheric heterogeneous chemistry have also become a significant research topic. Many more studies have focused on stratospheric aerosols<sup>18-25</sup> due to their effect on stratospheric ozone levels,<sup>26-29</sup> as well as their chemical simplicity compared with tropospheric particles. The stratospheric ozone layer protects life on earth from the sun's harmful ultraviolet radiation and has been affected greatly by heterogeneous chemistry between polar stratospheric clouds (PSCs) and gaseous halogen-containing species. These gaseous halogen species, such as  $\text{HCl}$  and  $\text{ClONO}_2$ , are produced by stratospheric photochemical reactions of anthropogenic emissions that include chlorofluorocarbons (CFCs). PSCs provide surfaces for these relatively

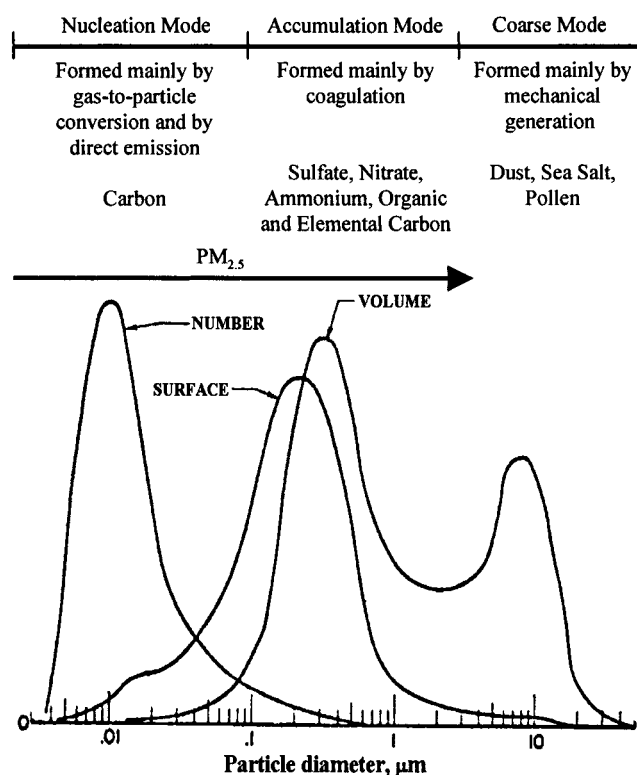


**Figure 1.** Illustrates a common urban aerosol distribution presented in number, surface, and volume distributions. Also, the three common aerosol modes (nucleation, accumulation and coarse) along with their main processes of formation and common sources and constituents are shown. (Reproduced and modified with permission from ref 33. Copyright 1982 John Wiley & Sons.)

unreactive species to undergo heterogeneous chemical processes to produce highly reactive halogen compounds such as  $\text{Cl}_2$ ,  $\text{HOCl}$ ,  $\text{BrCl}$ ,  $\text{HOBr}$ , and  $\text{Br}_2$  that can lead to reactions that destroy ozone catalytically. This understanding has led to the phase out of ozone depleting chemicals such as chlorofluorocarbons. Also, heterogeneous chemistry in the troposphere is of major importance<sup>30-32</sup> because life can directly be affected by chemicals and/or aerosols in this portion of the atmosphere. This makes the study of air pollution, gaseous as well as particulate anthropogenic emissions and their interactions between one other, an important area of current research.<sup>30</sup>

Conventionally, three ambient particle size modes exist<sup>33</sup> (see Figure 1). Particles less than approximately  $0.1\ \mu\text{m}$  belong to the nucleation mode and consist mainly of particles created from gas-to-particle conversion processes. Particles between about  $0.1$ – $2.5\ \mu\text{m}$  are considered to be part of the accumulation mode representing a region of particle growth mainly due to coagulation and condensation. Particles in both of these modes pose great health risks to humans because of their innate ability to deposit deep in the lungs. Larger, coarse mode aerosols greater than  $2.5\ \mu\text{m}$  are mechanically generated such as sea salt particles off the ocean or dust particles. Atmospheric lifetimes of nucleation mode and coarse mode particles are relatively short due to dry deposition mechanisms of Brownian motion and gravitational settling, respectively. The accumulation mode has no effective transport mechanisms and

**Table 1. Particle Mass Calculated for Different Particle Diameters**

particle diameter ( $\mu\text{m}$ )	particle mass ( $\text{g}$ ) <sup>a</sup>
0.01	5.2E-19
0.10	5.2E-16
1.00	5.2E-13
10.00	5.2E-10

<sup>a</sup> Assuming unit density spheres.

therefore has the longest atmospheric lifetimes from days to weeks unless scavenged by fog or precipitation.<sup>34</sup> Figure 1 shows a common urban aerosol showing plots of number, surface, and volume distributions. This illustrates that the majority of particles are located in the nucleation mode and the greatest surface area occurs in the accumulation mode while aerosol mass is divided between the accumulation and coarse modes. These concepts are basic, yet vital to solving atmospheric and biological questions related to single particles because different formation processes, chemistry, and health effects are associated with each of these modes.

In aerosol research, particulate matter has typically been studied using conventional sampling and analysis methods; however, a move toward on-line analysis with mass spectrometry (MS) has taken place. Conventional methods require collecting aerosols on filters for an allotted amount of time and performing off-line chemical analysis with such techniques as scanning electron microscopy (SEM), electron probe X-ray microanalysis (EPXMA), particle-induced X-ray emission (PIXE), atomic spectroscopy, high-performance liquid chromatography (HPLC), capillary gas chromatography (GC),<sup>35</sup> and ion chromatography (IC).<sup>36</sup> Mass spectrometry has also been used as an off-line technique utilizing laser microprobe mass spectrometry (LAMMS), secondary ion mass spectrometry (SIMS), and inductively coupled plasma mass spectrometry (ICPMS).

As mentioned above, aerosols cover an enormous size range from a few nanometers upward to about 100  $\mu\text{m}$ . This corresponds to subattogram to near microgram levels of material (See Table 1) with even smaller masses for individual components in heterogeneous ambient particles. Mass spectrometry has recently become a major contributor to the analytical aerosol community mainly for its high sensitivity and dynamic range, allowing for analysis over a wide range of sample mass. Interestingly, detection of small particles is not limited by mass spectrometer sensitivity but instead optical detection. This will be discussed thoroughly, (see Section IV) as will the progression toward on-line mass spectrometry of aerosols. This progression has involved the use of surface ionization with magnetic sector and quadrupole mass spectrometers and more recently laser desorption/ionization in conjunction with ion trap (ITMS) and time-of-flight mass spectrometers (TOFMS).

Throughout this aerosol mass spectrometry review, a number of acronyms are used, and Table 2 lists the most common along with their definitions. This paper provides a brief overview of relevant mass spectrometry instrumentation (see Section II). Subsequent

**Table 2. Acronyms Used Throughout This Review and Their Definitions**

acronym	definition
A TOFMS	aerosol time-of-flight MS
CAART	chemical analysis of aerosols in real time
DI	desorption/ionization
DIMS	direct-inlet MS
EI	electron impact
E OI D	electro-optical ion detector
HeNe	helium-neon
ICPMS	inductively coupled plasma MS
IP	ionization potential
ITMS	ion trap MS
LAMMS	laser microprobe MS
LAMPAS	laser mass analysis of particles in the airborne state
LDI	laser desorption/ionization
MALDI	matrix-assisted laser desorption/ionization
MCP	microchannel plate
MS	mass spectrometry/mass spectrometer
Nd:YAG	neodymium-yttrium aluminum garnet
PAH	polycyclic aromatic hydrocarbon
PALMS	particle analysis by laser MS
PAMS	particle analysis by MS
PM <sub>2.5</sub>	particulate matter $\leq 2.5 \mu\text{m}$
PMT	photomultiplier tube
PSPF	post source pulsed focusing
RSMS	rapid single-particle MS
SIMP	surface ionization monitor for particulates
SIMS	secondary ion MS
TOFMS	time-of-flight MS
USEPA	United States Environmental Protection Agency

sections furnish an overview of off-line chemical analysis of single particles (see Section III) as well as illustrate a comprehensive historical overview of on-line aerosol analysis by mass spectrometry through 1998 (see Section IV). The main focus of the review is on the instrumentation for the study of aerosols and the applications for which these instruments were designed.

## II. Aerosol Mass Spectrometry Overview

Aerosol MS instrumentation may be classified into several discrete sections: sample introduction, aerosol sizing techniques, ionization techniques, and mass spectrometer types. The importance of both sample introduction and sizing techniques will be discussed in conjunction with previous research on particle beams. This closely related research has assisted the field of aerosol mass spectrometry in many ways. The major advancements that have influenced the field of aerosol MS are discussed in this section, while the major instrumentation advancements when coupled to a mass spectrometer are discussed throughout the paper. Subsequently, ionization techniques and mass spectrometers are discussed. However, due to the vast amount of available information on each of these topics, only short overviews are given.

### A. Sample Introduction

Sample introduction methods are crucial in terms of single particle analysis because sample alteration must be kept to a minimum in order to obtain data that is representative of laboratory generated or ambient particles. Contamination and alteration, such as volatilization or crystallization, of substances are possible which can lead to false conclusions about original or "real particles." There have been major



advancements in this area ranging from physical placement of the sample into the ionization region of the mass spectrometer to introducing ambient particles on-line into the MS. Researchers outside the aerosol MS community have done much of this aerosol introduction work. Therefore, a brief discussion regarding this research is given focusing on particle beam characteristics, which are the basis for particle introduction into modern single particle mass spectrometers.

Particle beam research began with early instrumentation and characterization of particle beams<sup>37–43</sup> and is still making improvements that influence the introduction of aerosols into mass spectrometers.<sup>44,45</sup> A particle beam is formed when an aerosol expands through a capillary or converging nozzle into a vacuum. As the aerosol exits the nozzle, particles are accelerated by the bombardment of gas molecules. The gas molecules are subsequently removed by pumping, leaving particles that have a relatively large momentum to form a high speed particle beam. The maximum single particle velocity within this particle beam depends greatly upon the particle's size, mass, shape, and density with larger more massive particles traveling at slower velocities than less massive particles. Divergence is also an important characteristic of particle beams in which smaller, less massive, particles follow gas flow more than particles with greater mass. This leads to a greater beam divergence for smaller particles. Recently, aerodynamic lenses have been used to focus particle beams.<sup>44,45</sup> This sample introduction system allows for much greater particle transmission efficiency into the ion source region of a mass spectrometer. As will be seen (Section IV), each of these concepts have been used by many for the on-line introduction of aerosols.

## B. Aerosol Sizing Techniques

Precise determination of particle size is crucial because many aerosol properties and behaviors depend on their size.<sup>33</sup> Aerosol transport and atmospheric lifetime are related to gravitational settling and how well a particle will follow gas flow lines, which affects both ambient filter sampling as well as deposition in the respiratory system. As mentioned earlier, smaller particles can penetrate more deeply into the lung and are believed to be more pathogenic. Therefore, determination of particle size is essential when drawing conclusions about possible human risk associated with specific aerosols.

Because size is such an important particle characteristic, there have been developments in the aerosol MS community to not only collect mass spectra of particles but also determine their size. This combination of measurements has been done for years in off-line analysis, for example with LAMMS, by examining a single particle through a microscope and then obtaining the particle mass spectrum by laser desorption/ionization. After a particle beam is formed, there are many possible ways to obtain particle size information<sup>40</sup> of which single particle detection is the main goal. These include using one or two continuous wave lasers to either measure the light scattering intensity from single particles as they

pass through a single laser or measure the particles time-of-flight between two fixed position lasers. In either case, the scattered light intensity or the flight time can be related to particle size. (See Section IV-B-6 for more detail.) In many single particle mass spectrometers, these and other concepts have been utilized. Each specific on-line case will be discussed in detail (see Section IV).

## C. Ionization Techniques

Over the years, a variety of ionization techniques have been applied to particle analysis. These include inductively coupled plasma (ICP), secondary ion, surface or thermal, electron impact (EI), and laser desorption/ionization (LDI). Each of these techniques will be described briefly.

First, ICP is a high and uniform temperature continuous ionization source.<sup>46</sup> The plasma constitutes an extremely high-temperature ionized gas. It is produced by igniting a high flow rate of argon gas, which is surrounded by a water-cooled induction coil that is powered by a radio frequency (rf) generator. The resulting magnetic field, from the coil, interacts with the plasma in such a way that the ions and electrons move in a circular pattern within the coil. A plasma formed in this fashion allows for temperatures up to 10 000 K while resulting in temperature profiles much more uniform than other continuous sources such as flames and arcs. For these reasons, more complete ionization occurs which allows for lower detection limits and less chemical interference problems.

ICP is an ionization technique in which only elemental information is obtained. No molecular information, other than empirical formula, can be obtained as the plasma's thermal energy dissociates all molecules into their respective atoms, or atomic ions. Also, traditional sample introduction requires the dissolution of an aerosol from filter samples and subsequent nebulization into the plasma. This process not only leads to alteration of the original analyte but also limits aerosol analysis to bulk samples provided by filter extracts. (See Section III-A for more detail.)

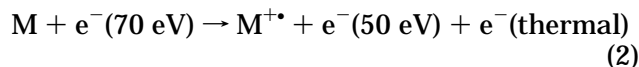
Secondary ion mass spectrometry<sup>46–48</sup> utilizes an ionization process, usually in conjunction with a microscope, in which detailed surface analysis is accomplished. It involves bombarding a solid sample with primary ions and mass analyzing the resulting ejected secondary ions. Primary ions<sup>49</sup> such as  $\text{Ar}^+$ ,  $\text{N}_2^+$ , or  $\text{Cs}^+$  are created in an ion gun by electron impact and then accelerated by a dc potential. Ion beams range in diameter between 0.3 and 5 mm and with ion focusing optics down to 1–2  $\mu\text{m}$ . Subsequently, these ions bombard the solid and strip off, or sputter, the surface layer of molecules or atoms. This bombardment causes the ejection of atoms and both positive and negative ions from the solid surface. These secondary ions are then directed into the MS by ion optics and mass analyzed. Moreover, SIMS is a surface analysis technique used for depth profiling<sup>50</sup> and is capable of depth resolution between 50 and 100 Å.<sup>46</sup> Due to the small beam diameter along with exemplary depth resolution, SIMS has been applied to off-line single particle analysis of filter samples.

Surface, or thermal, ionization requires a heated metal surface, usually rhenium, and produces ions according to the Saha–Langmuir equation<sup>51</sup>

$$\frac{n_+}{n_0} = \frac{g_+}{g_0} \frac{(1 - r_+)}{(1 - r_0)} \exp\left(\frac{\phi - IP}{RT}\right) \quad (1)$$

where  $n_+/n_0$  is the ratio of positive ions formed to neutral atoms,  $g_+/g_0$  is the ratio of the statistical weights of the ion and atom and has values on the order of unity. The value of  $\phi$  is the surface work function. IP is the ionization potential of the analyte, and  $r_+$  and  $r_0$  are reflection coefficients for ions and neutrals. In other words, this equation represents the relationship between incoming particles impacting the Re surface and leaving the filament either positively charged or as neutral desorbed ions. This ionization technique was used extensively in the first on-line single particle mass spectrometers. Its advantages and disadvantages are discussed later (see Section IV-A).

Electron impact ionization<sup>52</sup> occurs when an electron beam is created by a heated filament and directed through the source region where gaseous analyte atoms or molecules are present. These energetic electrons, usually with 70 eV of energy, are absorbed into the analyte's electron cloud. Using eq 2 as an example,<sup>52</sup> excess energy causes the analyte molecule, M, to eject a thermal electron as well as an electron of lesser energy. In this case, the analyte absorbs approximately 20 eV of kinetic energy.



The remaining 50 eV electron is then capable of interacting with either another analyte molecule or fragment ion and repeating this process. Therefore, the fragmentation process of the analyte depends on the amount of energy absorbed. The more absorbed energy, the greater the chance of fragmentation. For this reason, the fragmentation pattern is highly dependent on the energy of incident electrons and as a result, traditional electron impact utilizes electrons with 70 eV of kinetic energy.

EI requires that the analyte be in its gaseous state, which is difficult when applied to particles. Therefore, surface volatilization/ionization must precede EI in single particle analysis. We see later that when these methods are used in conjunction with one another (Section IV-A), they provide a more general particle ionization technique.

Finally, laser desorption/ionization requires a laser with a wavelength usually ranging from 10.6 to 193 nm. Lasers with such capabilities, used for particle analysis, include the CO<sub>2</sub> at 10.6  $\mu\text{m}$ , the neodymium-yttrium aluminum garnet (Nd:YAG), frequency quadrupled to 266 nm, and the excimer laser at 193 nm. The process involves a short laser pulse, in the 10 ns range for both the Nd:YAG and excimer lasers and 1  $\mu\text{s}$  range for the CO<sub>2</sub> laser, focused to a spot size between approximately 1  $\mu\text{m}$  and 1 mm, providing a laser fluence between 10<sup>6</sup> and 10<sup>12</sup> W cm<sup>-2</sup>.<sup>53</sup> When applied to particle analysis, the laser is either focused

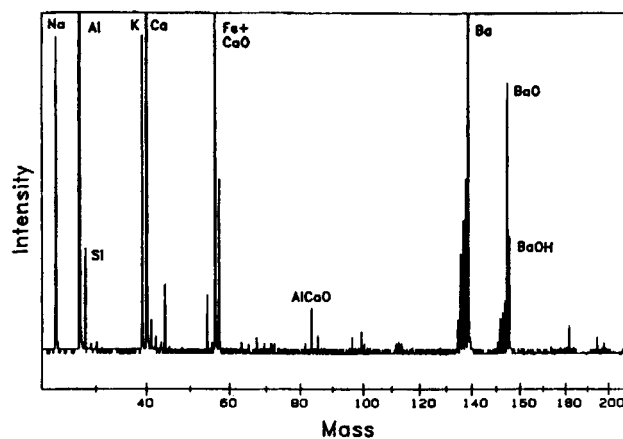


**Figure 2.** Portion of a positive ion LD mass spectrum obtained from a LAMMS system. (Reproduced with permission from ref 62. Copyright 1988 Elsevier Science.)

on a particle, as with LAMMS, or is triggered to fire at a single particle, as with on-line instruments. In either case, the particle absorbs photons and undergoes both desorption and ionization by the same pulse. Details of this process are still not completely understood; however, experimental evidence points in favor of a thermal process<sup>53–55</sup> as opposed to an electronic one.<sup>53</sup> A more detailed description of LDI including such processes as direct ionization of the solid, desorption/ionization (DI) of the solid immediately adjacent to the laser beam, gas-phase reactions within the microplasma and emission of neutral particles versus ion formation can be found elsewhere.<sup>56,57</sup> LDI not only depends on the substance's ionization potential and/or lattice energy<sup>58</sup> but also on the absorption cross section at the wavelength being utilized. In most cases, due to the high concentration of photons in these short pulses, multiple photons can be absorbed<sup>59</sup> by species in a particle. Moreover, there are two characteristic energy thresholds in LDI; the partial ionization and the plasma formation thresholds.<sup>60,61</sup> These represent the minimum and maximum amounts of energy needed to obtain useful information for particle analysis from the LDI process. During LDI of single particles, gaseous ions are formed which can be mass analyzed, most commonly with single particle analysis methods by using a TOFMS.

LDI can be applied to elemental, organic, molecular, and isotopic analysis.<sup>62</sup> First, much can be learned about elemental and molecular analysis by looking at a LDI spectrum, Figure 2, collected from a glass microsphere. This standard contains five major cations: silicon (16.9%), aluminum (7.5%), calcium (6.8%), iron (4.8%), and barium (2.5%). Interestingly, potassium is present in under 1% of the bulk in the particle. The spectrum illustrates some important characteristics about LDI. The intensities of both sodium and potassium illustrate an inherent high sensitivity toward alkali metals. The signal representing silicon is less than half the intensity of aluminum although silicon has an abundance greater than twice that of aluminum in this sample. It is important to understand that spectral intensities depend on the laser power density absorbed by the analyte as well as instrumental sen-

sitivity to the specific species. Variables that influence these include laser power, spot size, and absorption characteristics of the sample matrix and individual species present. Therefore, quantitation of LDI spectra is quite complicated due to the difference in sensitivity between species present in a particle as well as other factors such as reproducibility of laser power density absorbed from particle to particle. For organic analysis, high laser power tends to lead to extreme fragmentation of samples with lower powers causing less fragmentation and more parent ion formation. On the other hand, increased laser power leads to increased ion signal in inorganic analysis with the ionization threshold related to the ionization potential and/or lattice energy of the species under investigation. In this case, species determination is sometimes questionable, as reactions within the microplasma, or plume, during the LDI process are possible. Finally, isotopic analysis can be utilized with LDI. Although precisions and accuracies are not as high as SIMS, only a few percent, this might be a method of choice for elements that are not easily ionized with other methods.<sup>62</sup>

Laser desorption/ionization has distinct advantages when applied to aerosol analysis. First, LDI is ideally suited for on-line single particle mass spectrometry because the process is a fast, highly efficient vaporization and ionization technique that requires no sample preparation. Second, there are no artifacts from previous particles as is possible with surface ionization. Third, timing of the laser pulse works well with TOFMS analysis. Fourth, application of different power densities allows for different spectral characteristics to be enhanced or removed. Fifth, it allows for analysis of inorganic, organic, thermally labile, or relatively nonvolatile substances. Sixth, ionization characteristics can be used as a "fingerprint" for identification of many systems<sup>63,64</sup> as organic analysis has been done by LDI to ionize organic molecules with little fragmentation.<sup>63,65,66</sup> LDI is a powerful tool for the identification of the molecular species in a pure organic sample and in some cases identification can be obtained in mixed samples.

LDI has disadvantages associated with it also. First, shot-to-shot variations in power density and beam profile inhomogeneities can be dramatic, making quantitation a challenge. Second, reactions within the plume can form other species not present within the original sample. Third, preferential ionization is possible of material closest to the surface and to materials with either lower ionization potentials or better absorption characteristics at the chosen UV wavelength. Fourth, identification of organic molecules in complex heterogeneous ambient aerosols can be difficult due to the high abundance of organic fragments and species. Fifth, LDI mass spectra in many cases provide different fragmentation patterns when compared with other ionization techniques, such as EI. This can make qualitative determination of chemical species challenging. Despite these drawbacks, the many advantages of LDI make this a popular method of choice for ionization with real time single particle mass spectrometry techniques (see Section IV-B).

## D. Mass Spectrometers

Throughout the development of aerosol MS, different mass spectrometers have been utilized including magnetic sector, quadrupole, ion trap, and time-of-flight instruments. This section will briefly discuss each of these designs, as well as introduce their single particle analysis advantages and limitations.

Magnetic sector mass spectrometers apply a magnetic field that cause ions to form discrete, spatially separate ion packets according to their mass-to-charge ratio. These ion beams travel on slightly different trajectories through the instrument and are detected upon their exit from the magnet. Magnetic sectors are based on the following equation<sup>46</sup>

$$\frac{m}{z} = \frac{B^2 r^2 e}{2V} \quad (3)$$

where  $m/z$  is the mass-to-charge ratio,  $B$  is the magnetic field strength,  $r$  is the magnetic sector radius of curvature,  $e$  is the charge of an ion, and  $V$  is the acceleration voltage. In most cases, a magnetic sector instrument is used in conjunction with an electrostatic analyzer and is referred to as a double focusing MS. The magnetic sector directionally focuses the ions and the electrostatic analyzer accounts for differing kinetic energies resulting from ion formation. A mass spectrum is obtained by either scanning the magnetic field strength or the acceleration current while holding the other parameters constant. Different designs allow for ions to be either focused to a point or a focal plane. Therefore, depending on the configuration, a full spectrum is obtained by scanning or by the collection of ions with a photographic plate or a microchannel array detector. In either case, double focusing mass spectrometers can obtain high mass resolutions ( $m/\Delta m$ ) in the  $10^5$ – $10^6$  range.<sup>52</sup>

In terms of single particle analysis, magnetic sector instruments were utilized in the first on-line surface ionization instruments (see Section IV-A). Earlier versions utilized single magnets while a triple sector instrument, Figure 3, was put to use by Stoffels.<sup>67</sup> In the triple sector instrument, the first magnet provides a parallel ion focus in the vertical plane, the second provides a stigmatic focus, and the final electric sector maintains complete ion transmission. This configuration is referred to as a parallel/stigmatic/tandem (PST) arrangement and has been applied to isotopic analysis of elements, such as uranium, in single particles. In general, the use of magnetic sectors have been limited in single particle analysis by their scanning nature, as complete mass spectra cannot be obtained from a single particle. For this reason, magnetic sector instruments are not heavily utilized as aerosol analyzers today.

Quadrupole mass spectrometers are constructed of four cylindrical metal rods in which opposite pairs possess either a variable positive or negative dc potential. In addition, an ac potential is applied 180 degrees out of phase to these same rods. Ions are formed, typically by electron impact, extracted from the source and accelerated into the central region of the quadrupole. Both the ac and dc voltages affect



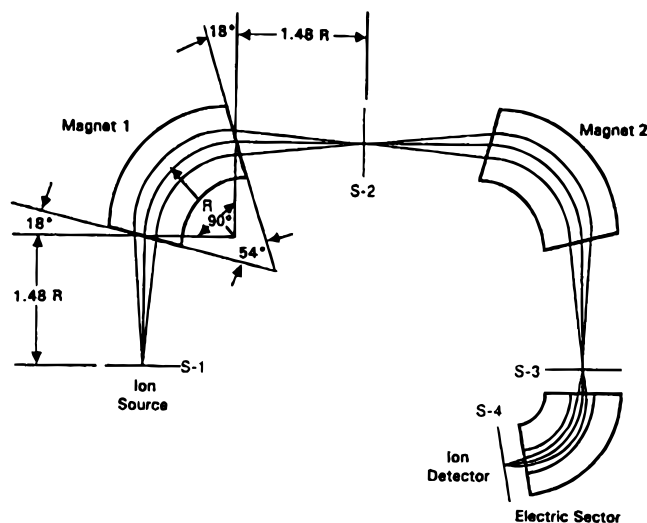


**Figure 3.** Ion optical design of Stöffels' double focusing, triple sector instrument. The first magnet provides a parallel ion beam in the vertical plane while the second magnet provides for a stigmatic focus. (Reproduced with permission from ref 67. Copyright 1994 Elsevier Science.)

the ion trajectories. Qualitatively, the quadrupole acts as a band-pass filter.<sup>46,68</sup> Consequently, only a certain  $m/z$  can obtain a stable ion trajectory and pass through the quadrupole to the detector. This occurs when an ion has a large enough mass not to be eliminated by the ac voltage, high mass filter, and a small enough mass not to be eliminated by the dc voltage, low mass filter. Variables that affect ion motions while in the quadrupole include the distance between rods, the magnitude of the ac and dc potentials, the ac frequency, and the mass, charge, and position of the ion. With a more detailed analysis, using the Mathieu equations,<sup>52,68,69</sup> stability diagrams can be obtained for ion trajectories which allow the passage of certain  $m/z$  ions through the quadrupole. Finally, complete spectra are obtained by scanning the  $m/z$  range of interest by increasing both the ac and dc voltages. Unfortunately, quadrupole mass spectrometers cannot be used to obtain a complete mass spectrum with single particle analysis as the time needed to scan the full mass range to obtain a full spectrum is too long. As will be seen later, the quadrupole mass analyzer was used with early on-line particle mass spectrometers (see Section IV-A), but has not been widely utilized in modern instruments due to its scanning limitations. Interestingly, it is beginning to be utilized to a greater extent once again (see Section IV-C).

Another type of MS utilized for particle analysis is the ion trap mass spectrometer. It consists of a doughnut-shaped ring electrode and two end cap electrodes that are usually at ground, but a fixed ac or dc voltage can be applied under certain circumstances. Ions are trapped when a variable radio frequency voltage is applied to the ring electrode. As the rf amplitude increases, larger ion orbits stabilize while smaller ions destabilize and collide with the ring electrode.<sup>46</sup> Similar to the quadrupole mass analyzer, the Mathieu equations describe ion motion within the ITMS.<sup>52</sup> This motion depends on the dc bias to the end caps, the angular frequency and potential, the radius of the ring electrode, and the

ion  $m/z$ . Depending on the potentials applied to these electrodes, many different experiments can be done. All ions within a designated  $m/z$  range can be trapped, and a complete mass spectrum taken by ramping up the rf voltage. As the ion orbits destabilize, they are ejected through an opening in an end cap and detected usually by an electron multiplier. Also, using a different configuration one specific  $m/z$  can be trapped. MS/MS can be accomplished by allowing this one trapped  $m/z$  to undergo collision-induced dissociation with a He bath gas that is always present<sup>70</sup> and subsequently collecting the mass spectrum of the fragment ions. This is a valuable tool for gaining additional chemical information and interpreting mass spectra. Figure 4 illustrates the configuration of the only on-line single particle instrument of this kind<sup>71</sup> (see Section IV-B-7).

A limitation of this technique applied to single particle analysis includes space charge effects.<sup>72,73</sup> Ion traps can only hold a certain number of ions until repulsive, or space charge, forces cause ion leakage. Space charge effects not only limit mass resolution as ion density increases but also can cause calibration problems and nonlinearity in instrument response. Therefore, this can be a major problem when applied to particles as ion signals covering orders of magnitude are produced.

Time-of-flight mass spectrometry is based on mass analysis of ions by flight times, or temporal separation. Ideally, after ionization all ions have the same kinetic energy. Therefore, ions of smaller mass will reach the detector, usually an electron multiplier detector or microchannel plate, with shorter flight times than ions of larger mass. TOFMS is based upon the following equation:

$$t = L \left( \frac{m}{2zV} \right)^{1/2} \quad (4)$$

where  $m/z$  is the ion's mass-to-charge ratio,  $V$  is the acceleration voltage of the ions,  $t$  is the ions flight time, and  $L$  is the length of the flight tube.<sup>59</sup> Advantages of TOFMS applied to particle analysis include the ability to obtain an entire spectrum on the order of microseconds while also having a theoretically unlimited mass range. On the contrary, only intermediate mass resolution on the order of  $10^3$  is routinely achieved for single particle analysis.<sup>52</sup> One reason for this relatively low resolution is due to the relationship  $m \propto t^2$ . As the mass increases, the separation in time decreases leading to poorer resolution at higher masses. Also, low resolution is caused by a range in flight times for the same  $m/z$  because not all ions have equal kinetic energies after their formation. Ions are formed not only at different times but also in different locations in the source and therefore undergo different accelerations, which lead to broader peaks and lower mass resolution.

With the use of either post source pulsed focusing (PSPF) or a reflectron, mass resolution can be increased.<sup>74</sup> PSPF focuses ion packets by applying an electric field for a short period of time between the source region and the flight tube. This allows for ions of the same  $m/z$  ratios to arrive at the detector at

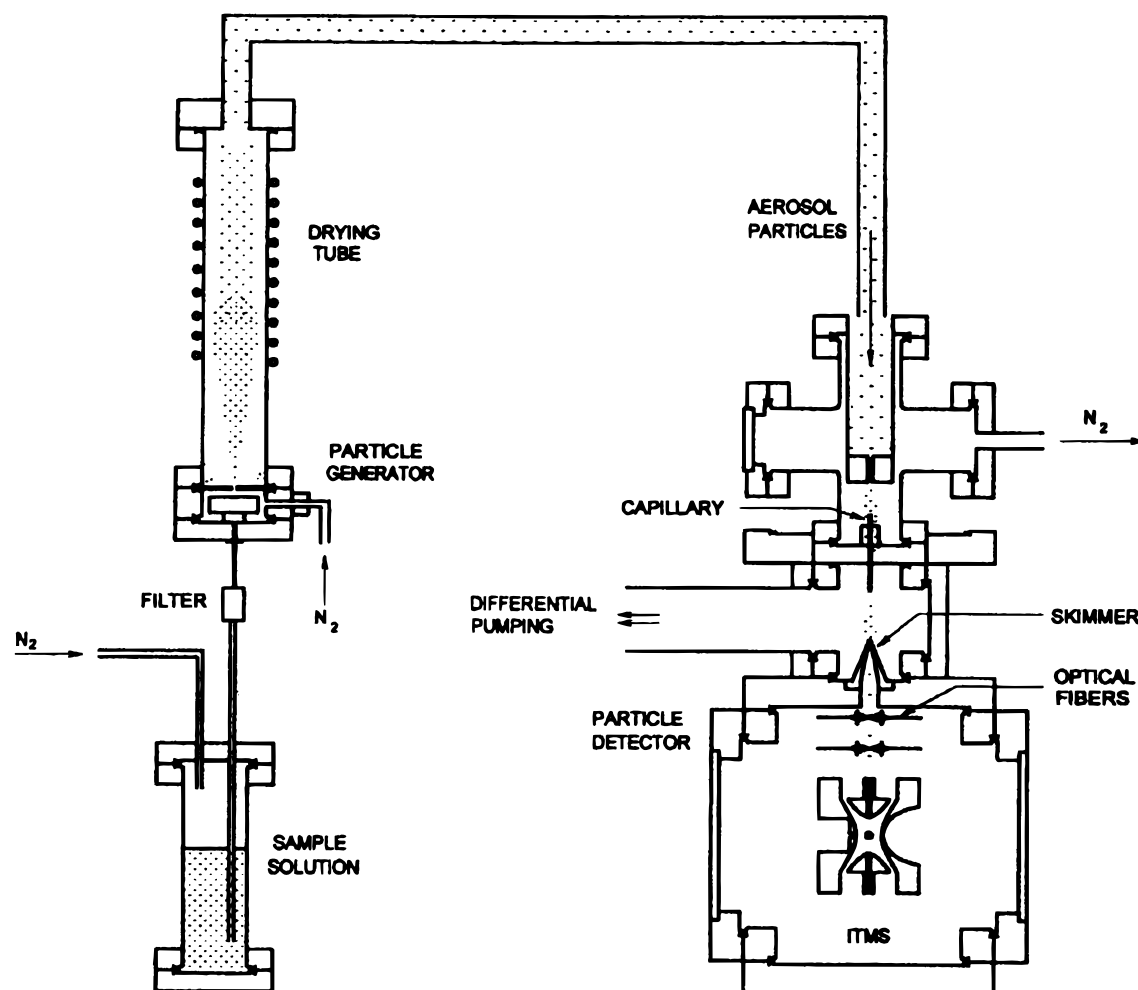


**Figure 4.** Experimental setup of Ramsey and Whitten's on-line ion trap aerosol mass spectrometer. MS/MS of single particles is accomplished with this design. (Reproduced with permission from ref 71. Copyright 1996 John Wiley & Sons.)

much closer times, leading to higher mass resolution. Unfortunately with PSPF, only a portion of a mass spectrum can be improved and calibration is more difficult because the ion's time-of-flight is not simply related to the square root of  $m/z$ . With the use of a reflectron, mass resolution is increased over the entire mass spectrum. The reflectron applies a deceleration field to the ions, which reverses the ions flight path back down the flight tube where they are detected. This compensates for different initial kinetic energies, or flight times in the drift region, by causing higher kinetic energy ions of the same  $m/z$  to penetrate farther into the reflectron. Therefore, ions of the same  $m/z$  ratio but different kinetic energies arrive at the detector at the same time increasing the mass resolution. Both PSPF and reflectron TOFMS have been applied to single particle analysis. However, the reflectron has found much greater application. Figure 5 illustrates the aerosol time-of-flight mass spectrometer (ATOFMS) which exemplifies the reflectron configuration<sup>75</sup> (see Section IV-B-6). In general, because of its speed, simplicity, high sensitivity and the ability to provide a complete mass spectrum of each individual particle, TOFMS has been the mass spectrometer of choice for recent on-line single particle mass spectrometers (see Section IV).

The four mass analysis techniques described in this section have been used throughout the development of aerosol mass spectrometry and all are being utilized today. This will be illustrated by an overview of off-line particle MS techniques (see Section III) as well as a comprehensive overview of on-line single particle analysis using mass spectrometry (see Section IV). The purpose of the following section is to illustrate the advantages and limitations of these off-line methods and describe the move toward on-line particle MS.

### III. Off-line MS of Aerosols

Aerosols have been studied off-line with the use of several mass spectrometry techniques. These include traditional surface analysis techniques such as LAMMS, SIMS, and an elemental analysis technique, ICPMS. Each of these methods has been utilized for off-line chemical analysis of traditionally sampled aerosols collected on filters or with cascade impactors. First, an instrumentation overview along with selected LAMMS applications is discussed. Next, applications of SIMS pertaining to particle analysis are described. In both cases, all experiments have been off-line and mainly for the quantitative determination of inorganic and qualitative analysis of nonvolatile organic aerosols. Recently, ICPMS is moving toward



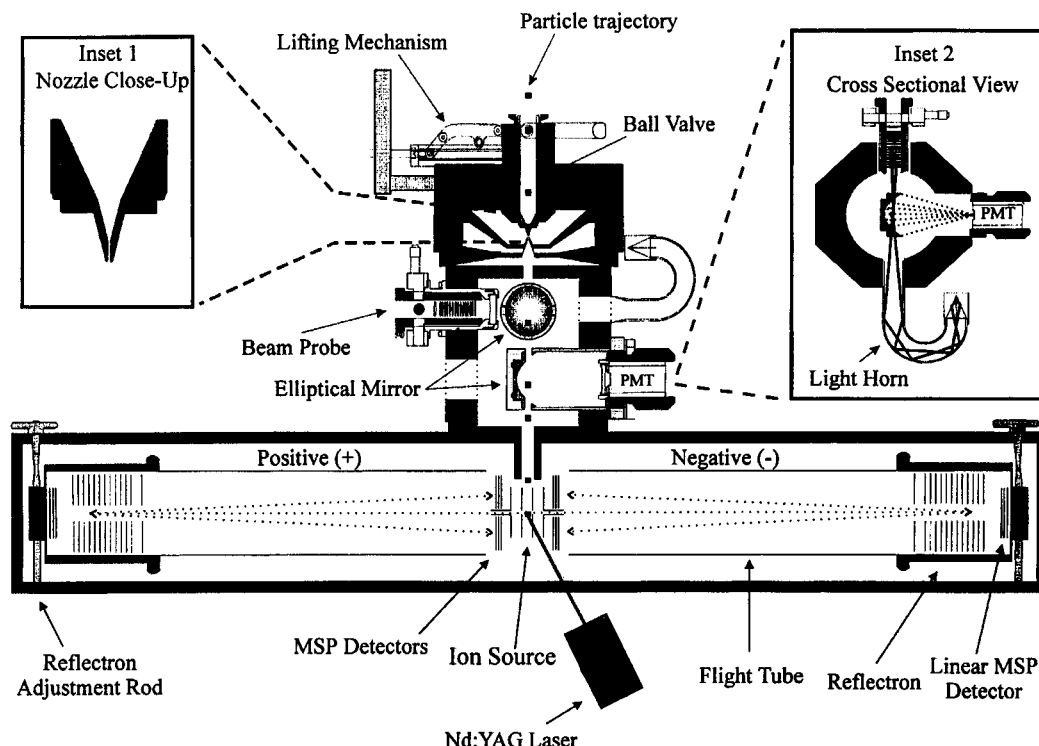


**Figure 5.** Schematic of Prather's dual polarity, on-line, field transportable TOFMS that acquires both positive and negative mass spectra for each single particle. (Reproduced with permission from ref 75. Copyright 1997 American Chemical Society.)

on-line particle analysis and its initial publications are introduced. Overall, this section illustrates the advantages of these techniques as well as disadvantages that have led aerosol research in the direction of on-line chemical analysis of single particles.

### A. Laser Microprobe Mass Spectrometry (LAMMS)

Many reviews of this field have already been published.<sup>62,63,76–79</sup> Therefore, a comprehensive overview is not our goal; instead our objective is to present an overview of the technique and how it is applied to aerosol research. First, LAMMS instrumentation is introduced illustrating the different possible configurations of commercial instruments as well as discussing common operating conditions. Next, LAMMS is evaluated in terms of advantages and limitations as applied to particle analysis. Finally, certain single particle applications are introduced, therefore excluding all surface analytical applications such as biologically related studies<sup>80–82</sup> and microanalysis of metal surfaces.<sup>83,84</sup> This should give the reader an appreciation for the importance of this method in the growth of several areas of aerosol research and technology.

LAMMS was developed in the 1970s with the first commercial instrument, the LAMMA 500, arriving in the late 1970s followed by the LAMMA 1000. These LAMMA instruments were first marketed by Leybold-Heraeus (Cologne, Germany) and now by SPECS (Berlin, Germany). Since then, other commercial instruments such as the LAMMA 2000 and LIMA 2A, produced by Kratos (Manchester, U.K.), are on the market. The basic instrumentation is very similar although they differ in configuration. Figure 6 illustrates the LIMA 2A.<sup>76</sup> Here, two lasers are

aligned collinearly to allow for visualization and desorption/ionization of the analytical sample area. A low power helium–neon (HeNe) laser is focused onto the sample and positioned by micromanipulators. After the analytical area is determined, most commonly a frequency quadrupled, 266 nm, Q-switched, Nd:YAG laser is focused to a spot size of 1–3  $\mu\text{m}$  on the analytical surface where LDI occurs. The UV laser applies controlled pulses of approximately 8 mJ for 5 ns to the surface while allowing for power densities between  $10^5$  and  $10^{11}$   $\text{W cm}^{-2}$ . A complete mass spectrum is obtained by a reflectron TOFMS after laser ablation, either representing positive or negative ions depending on the chosen instrument polarity.

The LIMA 2A instrument allows for both transmission and reflection sample analysis configurations, as illustrated in Figure 6. The transmission method relies on extremely thin sample thicknesses, on the order of a micrometer, and the collection of ions on the same axis yet on the opposite side of the sample. Common analytical samples include thin films, thin biological samples, and particles collected on a substrate, most commonly transmission electron microscope (TEM) grids. The LIMA 2A can also operate in a reflection configuration. In this case, the UV laser impacts the sample either perpendicularly or at an angle less than  $45^\circ$  from the perpendicular. In contrast to the transmission configuration, ions are then collected on the ablated side of the sample. Unlike this interchangeable instrument, the LAMMA 500 operates solely in transmission mode, while the LAMMA 1000 and LAMMA 2000 operate solely in the reflection mode. Moreover, Fourier transform mass spectrometry (FTMS) has been utilized in LAMMS;<sup>85–87</sup> however it has not been used to the

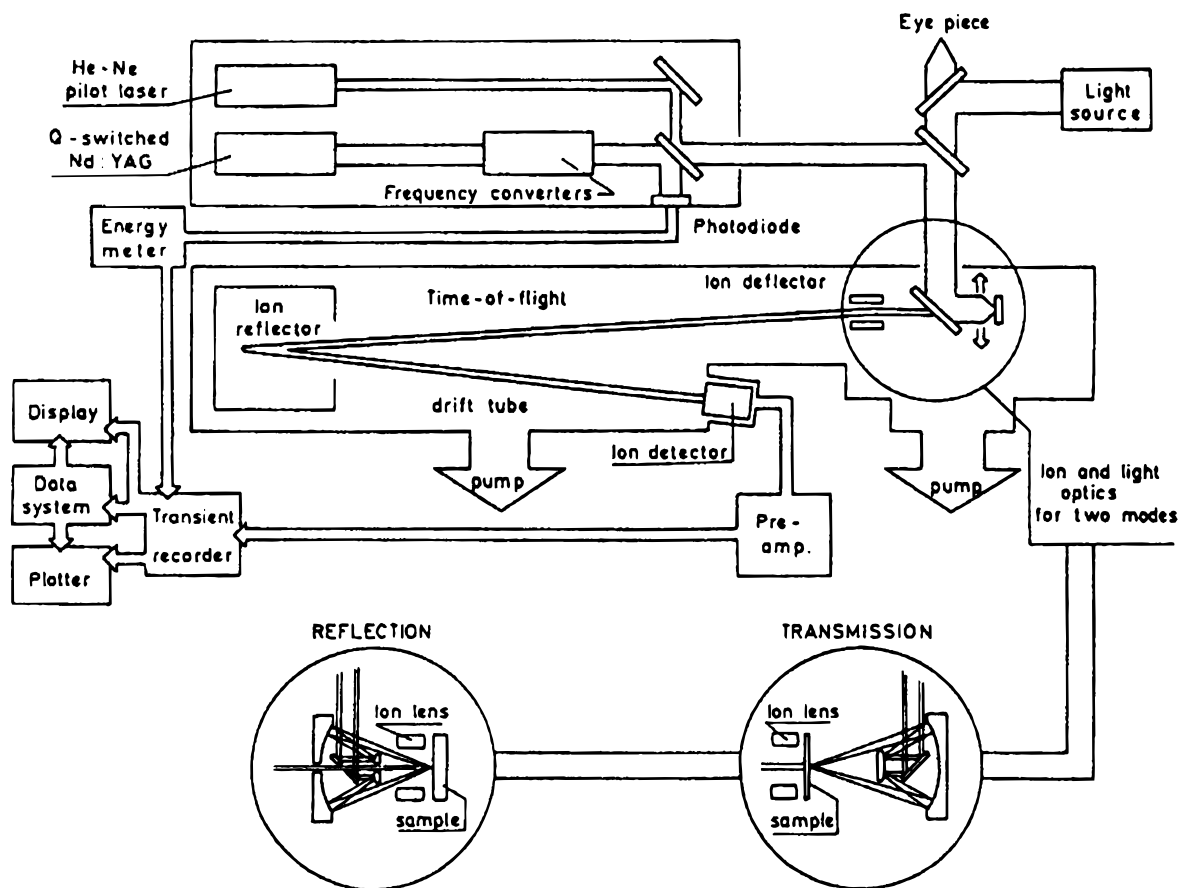


**Figure 6.** Schematic of LIMA 2A laser microprobe mass spectrometer with time-of-flight mass analyzer. Also emphasized are the reflection and transmission geometries. (Reproduced with permission from ref 76. Copyright 1994 John Wiley & Sons.)

extent of TOFMS and due to the overall objective of this section, FTMS will not be discussed.

LAMMS has certain operating requirements<sup>78</sup> that lead to both advantages and limitations. First, sample size and preparation is of obvious concern especially when dealing with transmission experiments.<sup>88</sup> Most commonly, preparation mirroring TEM is utilized for biological samples as well as other mechanically stable and extremely thin or small materials such as particles. The sample is then placed within the vacuum and subsequently analyzed. This analysis procedure can be as quick as 10–15 min. However, it is beneficial to obtain spectra at different power densities, in different polarities, with different surface areas as well as different depths of the sample. Most importantly, with this method multiple spectra can be obtained from individual particles. This is a definite advantage over on-line techniques where at most two spectra may be obtained (see Section IV-B).

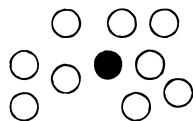
In these LAMMS systems, a TOFMS is utilized which allows for high transmission, therefore high sensitivity, adequate mass resolution and a complete mass spectrum per laser pulse. High ion transmission is extremely important because of the small number of ions produced. For example, in a 1  $\mu\text{m}$  spot size the amount of vaporized material is less than a picogram,  $10^{-12}$  g, which relates to formation of approximately  $10^5$  neutral atoms for a 1 ppm component with a molecular weight of 100.<sup>76</sup> To deter-

mine the number of detectable ions or transmission of the MS, estimates have been made that approximately 1 ion reaches the detector in a TOF LAMMS system for every  $10^3$ – $10^4$  atoms vaporized.<sup>76</sup> Moreover, the resolution,  $m/\Delta m$ , varies from 500 with the LIMA 2A to 4500 with the LAMMA 2000 for the lead isotopes at  $m/z$  206, 207, and 208.<sup>76</sup>

There are many advantages as well as disadvantages with these known operating criteria when applied to single particle analysis. First and foremost, the focusing optics allow for single particle analysis. This not only permits location but also laser ablation of a single particle. Second, sample preparation is relatively straightforward. Particles are most commonly collected on TEM grids in size segregated cuts within an impactor and subsequently introduced into the LAMMS. Third, utilizing a TOFMS allows for high transmission of ions and adequate mass resolution. Fourth, many nonvolatile or thermally labile compounds can be studied that could not be analyzed with other more conventional mass spectrometric techniques. Fifth, with the ability for inorganic and organic speciation, applications to ambient aerosols have been widespread.<sup>89–91</sup>

LAMMS suffers from some important limitations. First, sample collection and preparation lead to severe disadvantages. Collecting ambient particles on filters in impactors, over several hours, allows for size segregation, but time resolution is lost. In addition, these collected particles can change with time before

**EXOGEN MIXTURE:**  
10 Wt.-% quartz featuring  
10 Particle-% of pure quartz



**ENDOGEN MIXTURE:**  
10 Wt.-% quartz featuring  
0 Particle-% of pure quartz

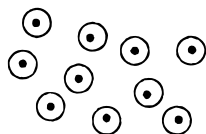


**Figure 7.** Model of a chemical species, 10 wt % quartz, determined by conventional bulk analysis, distributed in either an exogen, externally mixed, or endogen, internally mixed, manner. (Reproduced with permission from ref 97. Copyright 1993 Gordon and Breach Publishers.)

analysis. For example, semivolatile species can volatilize, water droplets collected can crystallize and/or evaporate depending on temperature and humidity conditions after collection, and particle–particle or gas–particle reactions can also take place. In any case, once the sample is within the mass spectrometer additional semivolatile species may be lost. Often, due to the submicrometer size range of some single particles, one laser pulse may ablate the entire particle. This is problematic because only a positive or negative spectrum can be obtained from a single particle. LDI also limits this technique (see Section II-C). Despite these limitations, the ability to study single particles is and has been extremely important. Next, some environmental LAMMS applications are examined to illustrate the importance of this technique to single particle research.

Many environmental applications have been reported as related to qualitative determination of particle types at various global locations. Urban pollution particles, lead containing<sup>92</sup> and environmental soot<sup>93</sup> particles, represent examples of what has been analyzed using this single particle approach. LAMMS was used to determine the inorganic and certain organic components in individual soot particles.<sup>93</sup> Polycyclic aromatic hydrocarbons were identified as they absorb well at 266 nm and form positive molecular ions where there are no spectral interferences. Other applications include monitoring Antarctic aerosol particles. These studies give information on particle types within each size bin from a cascade impactor<sup>91</sup> and seasonal behavior of certain components such as methanesulfonate, nitrate and metallic substances including barium and lead.<sup>89</sup> Other environmental samples include Amazon basin aerosols<sup>94</sup> and marine aerosols from such places as the North Sea<sup>90,95</sup> and the Brazilian coast.<sup>96</sup> Finally, the concept of homogeneous, internally mixed, versus heterogeneous, externally mixed, aerosols were studied with coal mine dusts.<sup>97</sup> This concept helps clarify the speciation among single particles from bulk aerosol measurements. As shown in Figure 7, the species of interest in an exogen mixture is present

in a pure particle, or mixed externally within an aerosol, while in an endogen mixture the component is distributed evenly, or mixed internally within the aerosol. Therefore, if bulk measurements are taken, it is unknown whether the species, quartz in this example, is distributed homogeneously or heterogeneously in the sampled aerosol. This coal mine study found that potentially toxic materials, silica and siderite, are typically found in exogen mixtures. Consequently, toxicological effects and possible removal or filtration of such species greatly depends on this knowledge. With this information along with other studies, possibly including particle size, an improvement of coal workers health may be made in the future. Therefore, studies employing LAMMS such as the ones mentioned earlier along with many other applications have added significantly to the field of aerosol MS.

## B. Secondary Ion Mass Spectrometry (SIMS)

Although this technique has been available for years, it has only recently been utilized for single particle research. SIMS is the only mass spectral technique that can be used to accurately depth profile single particles as it has a depth resolution of approximately 1 nm.<sup>98</sup> It also has the ability to obtain numerous mass spectra of both polarities from a single particle. This allows for observation of chemical constituents and heterogeneities associated with depth in a particle. SIMS also has the capability to detect all elements and can be used for isotope ratio measurements. On the other hand, this technique suffers from many of the same limitations as LAMMS. Both are off-line techniques and must rely on filter collection and sample preparation for aerosol analysis. Moreover, due to the short amount of time that SIMS has been applied to aerosol research, only a limited number of its advantages have been exploited. This section illustrates its recent applications and advancements to the aerosol field.

The primary ion beams for the following applications include  $\text{Cs}^+$ ,<sup>99</sup>  $\text{Ga}^+$ ,<sup>100,101</sup>  $\text{Ar}^+$ ,<sup>102</sup> or  $\text{ReO}_4^-$ ,<sup>100</sup> and the mass spectrometers include quadrupoles, TOF,<sup>100,101</sup> or an ion trap.<sup>100</sup>

Goshnick et al. used SIMS for depth profiling of laboratory generated salt samples that included chlorides, nitrates, sulfates, and carbonates, representing environmental materials.<sup>98,103</sup> Next, ambient aerosols were sampled near a highway in Germany.<sup>104</sup> Depth profiling of the samples showed that the particles have an inorganic core of ammonium sulfate, formed by an atmospheric reaction of ammonia and sulfuric acid. These particles appeared to be coated with a 200 nm organic layer, most likely from the aggregation of soot from car exhaust. Later, more detailed analysis of these particles allowed for the determination that they belonged to one of two types of aerosols. The organic and ammonium sulfate particles were mainly found in the submicron size range (0.2–1.2  $\mu\text{m}$ ) while coarse particles (1.2–3.7  $\mu\text{m}$ ) constituted mainly soil particles.<sup>101</sup> Moreover, this study utilized a TOFMS and reported complete positive and negative ion mass spectra of single particles. More recently, another field study located



in an area of considerable air pollution showed similar results, concluding that the surface composition depended little on air composition while having great dependence on source emissions. Again, it was found that carbon compounds dominated the outermost molecular layers of the aerosol.<sup>102</sup>

Van Grieken has also utilized SIMS for aerosol analysis.<sup>98</sup> Depth profiles on other urban aerosols showed the majority of aluminosilicates were covered with both vanadium and chromium. This combination of chemical species suggested that these were fly ash particles. Chrysotile asbestos fibers coated with titanium chloride were also examined.<sup>105</sup> Another surface fiber study, performed by Lancin et al., was accomplished illustrating the capability to apply depth profiling to the outermost layers of fibers.<sup>99</sup>

Finally, Nihei et al. introduced the gallium focused ion beam, Ga-FIB, which allows for better spatial resolution.<sup>98</sup> It has a beam diameter of less than 0.1  $\mu\text{m}$  that is not only superior to other ion beams but also allows analysis of submicron particles. Goshnick et al. and Groenewold et al. utilized this ion beam. Groenewold et al. compared the disappearance cross section, or material removed, utilizing  $\text{Ga}^+$  as the primary ion beam with that obtained using  $\text{ReO}_4^-$ .<sup>100</sup> This was accomplished by coupling this ionization technique separately to a quadrupole, an ion trap, and a TOFMS. They found, not only was the disappearance cross section less for the monatomic ion beam but it was also less for a fluid surface, gelatin, than a refractory solid surface, silicate. Also, the detection limit was estimated for tetraethylammonium ( $\text{TEN}^+$ ) on soil using  $\text{ReO}_4^-$  with the quadrupole to be about 500 ppb. This result suggests that lower detection limits should be possible with a brighter primary ion beam and/or an ITMS.

### C. Inductively Coupled Plasma Mass Spectrometry (ICPMS)

This elemental ionization technique is relatively new to single particle research. Only two research groups, Jalkanen and Hasanen from Helsinki, Finland, and Kawaguchi et al. from Nagoya University, Japan, have published applications involving aerosol analysis. In both applications, quadrupole MS instruments are utilized. Results from each of these groups are discussed below.

First, Jalkanen and Hasanen developed a simple method for the dissolution of atmospheric aerosol filter samples (see Section III-A for limitations) for bulk analysis by ICPMS.<sup>106</sup> This off-line method was shown to be quantitative for all elements in the National Institute of Standards and Technology (NIST) Standard Reference Material (SRM) 1633a Coal Fly Ash. Afterward, this method was applied to quantify specific elements including Al, Mn, Na, and V in ambient samples.

Kawaguchi et al. do not use ICPMS with filter samples but instead introduce aerosols directly into the ICP.<sup>107</sup> This leads to a single ion pulse for each particle with a height corresponding to the amount of each analyte element. They have showed calibration results for both zinc and lead single particles produced by a vibrating orifice monodisperse aerosol

generator. In both cases relatively broad pulse-height distributions were found for monodisperse aerosols which lead to higher detection limits than ICP-AES. However, after optimization of such parameters as carrier gas flow rate, radio frequency power, and sampling depth, detection limits for zinc were appreciably lowered.<sup>108</sup> The detection limits were determined to be 0.3 fg for lead in a monodisperse lead nitrate aerosol and 3 fg for zinc in a monodisperse zinc acetate aerosol.<sup>107,108</sup> In either case, these detection limits should both be appropriate for the analysis of inorganic species in ambient aerosols. Studies on ambient particles have not yet been conducted, however, this application has made a definite move toward on-line analysis utilizing ICPMS.

### IV. On-line MS of Aerosols

Knowledge of the advantages and limitations from off-line analysis of aerosols has led the aerosol field to modern on-line methods utilizing mass spectrometry. The main driving forces include limitations due to filter sampling and severe loss of time resolution with off-line methods. In contrast, on-line methods allow for observation of single particles on a real time basis. This move toward on-line MS of aerosols has been relatively recent but there are a number of reviews on research in this field.<sup>109–111</sup> The focus of this section is to follow the progression of on-line single particle analysis using mass spectrometry, providing a comprehensive review through 1998. The most effective way to accomplish this is to follow chronologically the development and subsequent improvement in this field, beginning with Davis and surface ionization studies in 1973 to laser desorption studies of the present day.

#### A. Surface/Thermal Ionization Mass Spectrometry

##### 1. Davis (1973)

Davis began the on-line chemical analysis of single particles in 1973 with a surface ionization magnetic sector mass spectrometer<sup>112</sup> illustrated in Figure 8.<sup>51</sup>

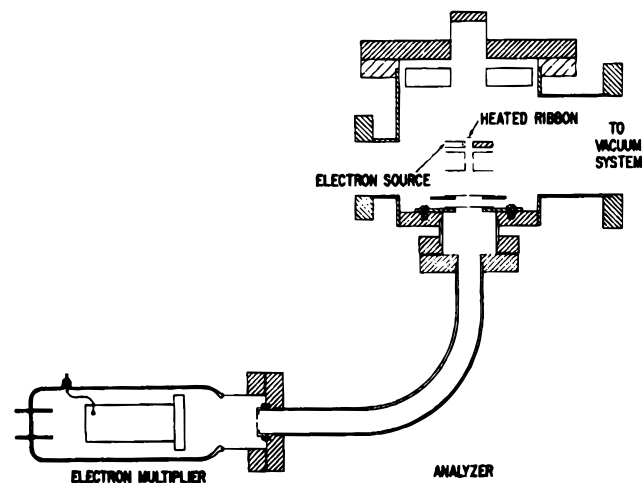


**Figure 8.** Schematic of the first aerosol mass spectrometer. This design, by Davis, utilized a heated rhenium ribbon for surface/thermal ionization and a single magnetic sector for mass analysis. (Reproduced with permission from ref 51. Copyright 1977 American Chemical Society.)

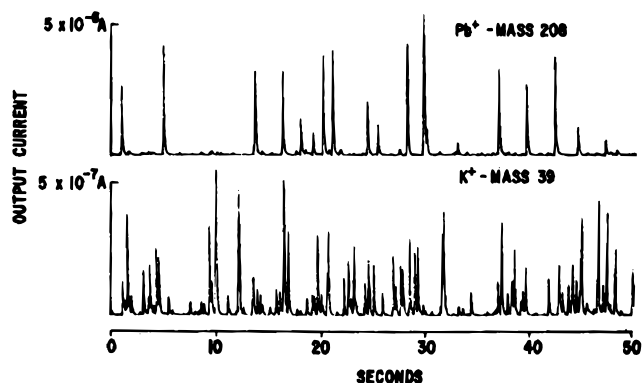


**Figure 9.** Illustrates typical output signals from surface ionization mass spectrometers. Here,  $\text{Pb}^+$  and  $\text{K}^+$  were monitored from laboratory air particles as each ion burst represents a particle that contained either lead or potassium. (Reproduced with permission from ref 51. Copyright 1977 American Chemical Society.)

This instrument allowed for the introduction of particles through a needle valve into the mass spectrometric region where the particles were ionized by a heated rhenium ribbon according to the Saha–Langmuir equation, eq 1, and mass analyzed by a 3-in. magnetic sector mass spectrometer. Each particle gave off a burst of ions, Figure 9, which could be monitored, counted, and related to the amount of an element in a particle. This illustrates the type of information Davis, as well as all other surface ionization researchers, obtained in these early particle studies.

Davis' applications mainly focused on instrument characterization and optimization. First, he decided on a rhenium filament rather than tungsten due to its superior performance.<sup>51</sup> He also determined that the work function of the metal increased with oxygen adsorption, or oxygen pressure, to the rhenium surface and decreased with temperature. Experimentally, he found an optimum operating temperature between 800 and 1500 K, depending on the elements under investigation, and a maximum in the work function of rhenium due to oxygen adsorption at  $10^{-5}$  Torr of about 7.2 eV at 1000 K.<sup>51</sup> This allowed for analysis of elements with ionization potentials up to approximately 8 eV.

Davis also reported single particle data.<sup>51</sup> He analyzed metals, such as Li, Na, K, Rb, Cs, U, Cr, Pb, and Cu, and depending on the ionization potential (IP) for each element a different ionization efficiency was determined. Due to lithium's low IP of 5.4 eV, a 100% ionization efficiency of small particles was observed. This allowed for detection of 800 atoms of  $\text{LiCO}_3$ , or a calculated particle diameter of 4 nm. In contrast, Cu having the highest IP examined of 7.7 eV emitted only 0.02% ions. To detect Cu in  $\text{CuO}$ ,  $7 \times 10^6$  atoms or a minimum particle size of 60 nm must be present.

Laboratory air results were presented for elements such as Pb, Cu, and Li.<sup>113</sup> Particles were collected on a cold filament for approximately 1 min and then quickly vaporized to produce a burst of ions. The output current of each particle's ions over time was recorded and from the known ionization efficiencies for each element, among other things, average lab

air concentrations were calculated. Furthermore, mass spectra of room air versus room air contaminated with cigarette smoke were obtained.

Davis' technique has several limitations. Particle size could only be determined for chemically homogeneous particles. Most importantly, this was not a universal method. Only particles containing elements with ionization potentials less than approximately 8 eV could be analyzed, thereby excluding many elements. Despite these limitations, Davis clearly illustrated that real time single particle mass spectrometry could be accomplished as he began the exciting field of on-line single particle mass spectrometry.

## 2. Lassiter and Moen (1974)<sup>114</sup>

One year after Davis introduced the technique, Lassiter and Moen introduced the quadrupole mass spectrometer for the use of particle analysis. The authors showed mass spectra of the system's background, laboratory air, and numerous powders. Most importantly, they illustrated that oxygen in the presence of a rhenium filament and a relatively high temperature, 800–1600 °C, raised the work function of the ribbon to a point that allowed for characterization of compounds that could not be analyzed without oxygen present.

## 3. Myers and Fite, SIMP (1975)

Myers and Fite developed an instrument based upon surface ionization with slight modifications.<sup>115,116</sup> In this case, particles were drawn in through a pinhole, passed through a skimmer, and directed to a heated metal filament: oxidized tungsten, for positive ions, or iridium, for negative ions. After surface ionization, a quadrupole mass spectrometer was used to mass analyze the focused ions. The output of the quadrupole was then sent to an ion multiplier where the signal was analyzed for peak height, shape, and count rate.

Although the instrument was similar to earlier designs, Myers and Fite's instrumentation was based on a different premise. They concentrated on the fact that sodium and potassium are the sixth and seventh most abundant elements in the earth's crust.<sup>115,116</sup> Consequently, they are present as impurities almost everywhere. They understood that if a particle made contact with their heated metal surface, pyrolyzed, and contained either Na or K as a major constituent or as an impurity, surface ionization would occur.

Myers and Fite contributed numerous advancements to this new field of single particle MS analysis. Interestingly, they showed that a rubidium oven could be placed before the ionization surface in such a manner that rubidium atoms would collide and stick to particles. Because rubidium has the second lowest ionization potential, their instrument's particle size detection limit was lowered to a few hundred angstroms.<sup>116</sup> Moreover, they utilized negative ion surface ionization. This occurs when the electron affinity of an element is comparable to the surface work function.<sup>115</sup> A thorium-coated iridium filament was used as it possesses a low work function of 2.7 eV and is conducive to negative ion formation.

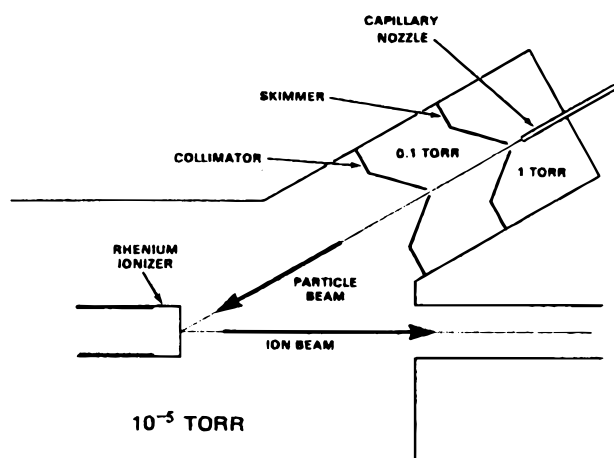


**Figure 10.** Schematic of Stoffels direct air sampling inlet for use in a surface ionization mass spectrometer. This design was also the basis for sample introduction in all modern on-line aerosol mass spectrometers. (Reproduced with permission from ref 117. Copyright 1981 Elsevier Science.)

They found that particles containing halogens, nitrate, and CN produced measurable signals.<sup>116</sup> A major interest involved counting particles containing either Na or K. As a result, they created a surface ionization monitor for particulates (SIMP) that strictly counted particles.<sup>115,116</sup> This instrument was used to monitor ambient particulate levels in Pittsburgh as well as in the stratosphere.

#### 4. Stoffels, DIMS (1981)

Stoffels developed the direct-inlet mass spectrometer (DIMS).<sup>117</sup> The particle inlet system, illustrated in Figure 10 based on earlier designs (see Section II-A), samples particles through a capillary nozzle operated at a critical flow rate of  $0.5 \text{ L min}^{-1}$ . The gas molecules reach sonic velocities which upon exiting the nozzle accelerate particles to similar speeds. Next, the aerosols travel through a skimmer and then a collimator. The skimmer diverts most of the gas while transmitting the particle beam and the collimator is used mainly to achieve another stage of differential pumping. Approximate operating pressures for each section were: nozzle-skimmer (1 Torr), skimmer-collimator (0.1 Torr), and source chamber ( $10^{-5}$  Torr).<sup>118</sup> Finally, the particles reach the rhenium filament where surface ionization occurs. The resulting ions are focused and accelerated into the magnetic sector mass spectrometer, the later model represented in Figure 3, by an electrostatic lens and detected by a Daly ion/electron/scintillation converter.<sup>119</sup> This ion detection system is utilized for its wide dynamic range leading to particle detection over the size range of about 5 nm to  $5 \mu\text{m}$ . Similar to previous instruments, a burst of ions is produced from each particle, which can be counted and related to the amount and type of component in the particle.

A thorough analysis of the interface region was performed including nozzle and transmission studies.<sup>118</sup> It was shown that smaller particles having less inertia follow gas flow lines and diverge more than larger particles. Therefore, divergence angle decreases with increasing particle size. Consequently,

transmission efficiency also depends on particle size. Stoffels used cesium nitrate particles with varying diameters to illustrate that transmission efficiency increased with increasing particle diameter.<sup>118,120</sup>

Stoffels presented a detailed analysis of real time particle measurements examining ion emission rates, particle size measurements, ion yields, and particle bounce.<sup>117</sup> Similar to others, he showed that at lower temperatures ion emission rates were on the order of minutes and represented groups of particles. As the filament temperature increased, single particle data were resolved, as ion bursts in tens of milliseconds were observed. Particle size characteristics were studied with different size monodisperse cesium nitrate aerosols. Stoffels showed that particle size could be determined from the number of ions produced per particle as a laser aerosol spectrometer was used for particle size verification. However, size information could only be determined for homogeneous particles and ion yield per particle for  $\text{Cs}^+$  was found to be proportional to surface area, not volume or mass. Finally, Stoffels overcame the particle bounce problem associated with larger particles by using a triangular oven ionizer. Particles entered through a 1 mm entrance and were able to collide with the walls many times to fully ionize the particle. This oven was tested with  $10 \mu\text{m}$  diameter particles and gave the ion yield which was expected for that particle size.<sup>117</sup>

Unlike Myers and Fite, and Lassiter and Moen, Stoffels relied on a magnetic sector mass spectrometer due to its dispersive nature and therefore superior isotope sensitivity. This is crucial in determining isotope ratios of radioactive elements. Moreover, the instrument's isotope abundance sensitivity was increased 2 orders of magnitude over other similar instruments by applying a unique ion focusing technique<sup>121</sup> and a triple magnetic sector mass spectrometer with nearly 100% transmission efficiency.<sup>67,122</sup> This newly improved instrument was used to analyze isotopic ratios of plutonium, iodine, and uranium at the Hanford site in Washington State.<sup>123</sup> Stoffels illustrated that uranium analysis could be done on single particles using particle inlet MS (PIMS) without isolating the uranium from heterogeneous particulate samples.

#### 5. Allen and Gould, CAART (1981)<sup>124</sup>

Chemical analysis of aerosols in real time, CAART, was designed to sample particles through a capillary nozzle, a skimmer, and a collimator. The resulting particle beam then entered a vaporizer-ionizer cell (VIC) which consisted of a conical coil tantalum wire filament. This filament, operated at about 1500 K, was specifically used for vaporization. The particles were subsequently ionized with electron bombardment, extracted, and focused into a quadrupole mass spectrometer. This instrument's detection efficiency was approximately 1 particle in 240 for  $0.5 \mu\text{m}$  particles and was used to analyze both inorganic and organic aerosols.

#### 6. Sinha and Friedlander, PAMS (1982)

The instrument designed and built by Sinha and Friedlander consisted of a capillary nozzle, two



skimmers, and a Re V-type filament which allowed for multiple collisions and therefore more efficient vaporization of individual particles.<sup>125</sup> From prior knowledge<sup>112,116,117</sup> showing that using a filament for the ionization process limited chemical analysis to compounds having ionization potentials of about 8 eV, electron impact was used in conjunction with conventional thermal volatilization, similar to Allen and Gould.<sup>124</sup> Therefore, particle analysis by quadrupole MS, PAMS, allowed for analysis of more compounds with higher ionization potentials. Also, particle bounce during solid analyses was solved by utilizing a Knudsen cell oven for complete volatilization which allowed for mass quantitation of NaCl particles.<sup>126</sup> More recently, Sinha has developed a miniaturized focal plane magnetic sector to be used as a field portable instrument<sup>127</sup> as well as an electrooptical ion detector (EIOD) which allows for the acquisition of all ions from a single particle.<sup>128</sup>

Sinha and Friedlander's main applications involved instrumental characterization and development and the analysis of biological compounds and sodium containing particles. First, transmission efficiency was determined to be size dependent with 2.77  $\mu\text{m}$  PSLs transmitting 35–50%. Also, a linear relationship between particle volume and MS signal intensity was found for various compounds such as glutaric acid and ammonium sulfate.<sup>125</sup> Second, mass spectra were obtained for several biological samples such as *pseudomonas putida* and *bacillus cereus*.<sup>129,130</sup> In each of these cases only partial spectra, approximately 30 ion peaks, were obtained of multiple particles upon scanning the quadrupole MS. Third, sodium chloride monodisperse particles were analyzed with a calibration curve obtained.<sup>126</sup> Afterward, mass analysis was accomplished for laboratory-generated NaCl particles, in a polydisperse aerosol on a real time basis<sup>131</sup> and subsequently, ambient NaCl particles were studied.<sup>132</sup> Particle numbers of NaCl-containing particles were determined to vary depending on the time of day and meteorological conditions such as wind direction and the presence of fog. Mass was calculated from the  $\text{Na}^+$  MS signal intensity assuming the particles were solid, spherical, and completely NaCl. These ambient findings illustrated that the highest number of Na containing particles were less than 0.4  $\mu\text{m}$  while nearly all the ambient Na mass was found within fewer particles greater than 1  $\mu\text{m}$  (see Figure 1).

Much progress has been made in the field of on-line surface volatilization/ionization aerosol mass spectrometry. By combining knowledge from previous particle beam research (see Section II-A) with mass spectrometry, the on-line introduction of single particles into the source region of a mass spectrometer was accomplished. This allows for determination of real time chemical information regarding aerosols. As will be seen, this knowledge of utilizing a nozzle to accelerate the particles and skimmers to allow for acceptable mass spectrometric pressures is utilized in nearly every modern aerosol MS.

On-line surface ionization MS techniques overcame the major limitation of off-line filter sampling and subsequent MS analysis, but still suffer from inher-

ent limitations. First, surface ionization mainly operates under the assumption that each aerosol is comprised of a single compound for both size and mass determinations. This is an acceptable assumption when using laboratory generated particles, but is unrealistic when applied to ambient particles. In addition, another main limitation is the utilization of scanning mass spectrometers that have an inherent inability to acquire an entire mass spectrum for single particles. To acquire a complete spectrum for a single particle, the majority of researchers in the on-line MS aerosol community have chosen to move in the direction of time-of-flight mass spectrometers in conjunction with laser desorption/ionization.

## B. Laser Desorption/Ionization Mass Spectrometry

Just as surface ionization played a role in advancing on-line analysis of particles, LDI is currently playing an even larger role in advancing this new mass spectrometry field. Much was learned from surface ionization researchers, however, unlike these early on-line instruments this section focuses on instruments utilizing LDI as well as different mass analyzers. The utilization of a laser for desorption/ionization of single particles occurred because of the many advantages associated with LDI (see Section II-C). This modern field has also moved away from the magnetic sector and quadrupole mass spectrometers and mainly utilizes time-of-flight mass spectrometry due to the ability to provide a complete mass spectrum per particle. Aerosol laser desorption/ionization MS has made exceptional instrumental improvements in the 1990s and has just begun tapping the immense body of possible applications. This section gives a comprehensive review of not only the instrumentation utilized with this technique but also the applications in this field through 1998.

### 1. Sinha (1984)

Sinha first introduced laser desorption/ionization to single particle mass spectrometry in 1984 with the use of a Nd:YAG laser. The overall apparatus consists of a particle sizing region as well as a mass spectrometer to monitor specific ions. Figure 11 illustrates the major sections consisting of the particle inlet, the sizing region and the MS source region.<sup>133</sup> The entire instrument includes an aerosol beam generator, which consists of a capillary nozzle and skimmer, two continuous wave HeNe lasers, located at known distances used to measure the particles velocities, a high-energy pulsed ionization laser, an electronic circuit to size particles and externally fire the Nd:YAG, and a quadrupole MS. After known monodisperse aerosols are introduced through the nozzle and skimmer, a particle scatters light from the first HeNe laser and is detected by a photomultiplier tube (PMT). This starts a clock on the circuit. The particle then traverses to the second laser and this scattered light stops the clock. The time between these two events is the particle's flight time, which is related to aerodynamic particle size. A calibration curve for aerodynamic particle diameter versus particle velocity was determined.<sup>133</sup> The circuit uses a

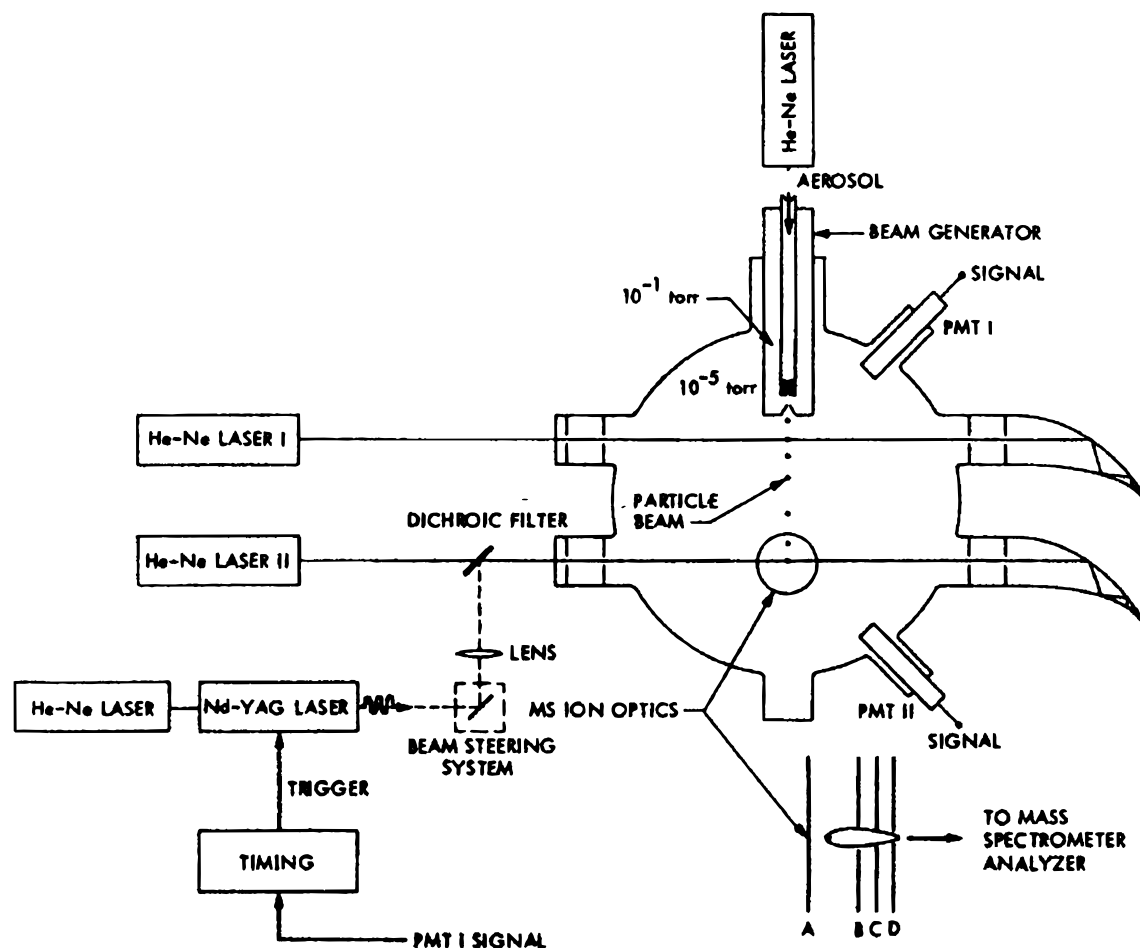


**Figure 11.** Sinha's experimental setup for on-line laser/desorption ionization. This design utilized a particle beam generator, two continuous wave HeNe lasers, and a Nd:YAG laser for DI. The particle beam traveled in the vertical direction while the quadrupole mass spectrometer and each of the lasers are perpendicular to this axis. (Reproduced with permission from ref 133. Copyright 1984 American Institute of Physics.)

light scattering signal from the first continuous wave laser and a delay generator, with an optimum delay chosen based on a single particle size/velocity. This delay accounts for the flight time of the particle to reach the location of the Nd:YAG pulse as well as for the time needed for the pulse to arrive after the laser is triggered. At this appropriate time, the circuit externally triggers the Nd:YAG laser, which is aligned collinearly with the second HeNe laser, to desorb and ionize the particle of interest. The DI laser produces approximately 1 J of energy for each 100  $\mu$ s pulse and is focused to a spot size of approximately 2.5 mm. This equates to a power density of only  $2 \times 10^5$  W  $\text{cm}^{-2}$ ,<sup>133</sup> which is too low for general analysis of organic molecules. Consequently, when potassium bipthalate was analyzed, only signals from potassium, CO fragments of the carboxylic groups and sodium, an impurity, were obtained. Also, the mass spectral efficiency, including vaporization, ionization and detection, was determined to be about  $10^{-6}$ , which corresponds to the detection of 1 in every  $10^6$  molecules in each particle.<sup>133</sup> Because of the disadvantages of the quadrupole, in 1991 Sinha utilized both the magnetic sector instrument and the EOID developed earlier.<sup>134</sup> This allows for the acquisition of an entire mass spectrum for a single particle ionized by LDI.

## 2. Marijnissen (1988)<sup>135</sup>

In 1988 a new design of aerosol MS instrumentation was proposed implementing a time-of-flight mass spectrometer with several lasers. The proposed instrument consisted of a capillary nozzle for the introduction of aerosols and a low energy laser to provide size information and instantaneously trigger the DI laser. Another UV laser to enhance the ionization would follow this step. A complete mass spectrum of these ions would then be obtained with a TOFMS.

Proposed applications were to compare the reproducibility of mass spectra from this technique to LAMMS. Other proposed applications included instrumental optimization, collection of data as a function of particle size to monitor ambient aerosols and to observe particle formation and other dynamic processes over time. (See Section IV-C for current published instrument.)

## 3. Johnston and Murphy (1991)<sup>136</sup>

These researchers grouped previous successful ideas and applied them to the first on-line laser desorption ionization time-of-flight mass spectrometer utilized for single particle analysis. This instrument consists of a differentially pumped particle

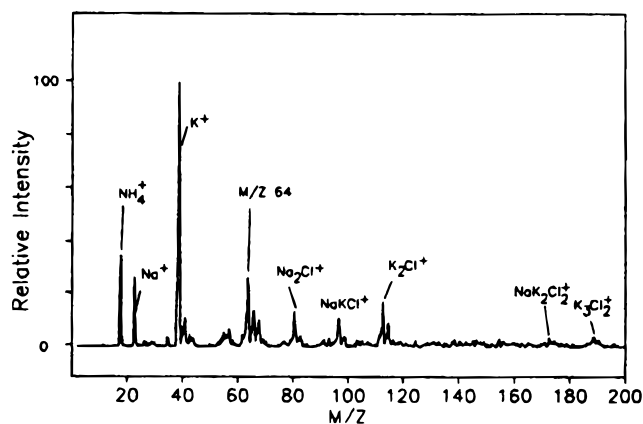


**Figure 12.** First on-line laser desorption/ionization single particle time-of-flight mass spectrum. This was a  $9\ \mu\text{m}$  particle consisting of  $(\text{NH}_4)_2\text{SO}_4$ ,  $\text{KCl}$ , and  $\text{NaCl}$  in a 1.6:1.0:3.6 mole ratio. (Reproduced with permission from ref 136. Copyright 1991 American Chemical Society.)

inlet, a single HeNe laser, an excimer laser, and a time-of-flight MS. Particles are accelerated through the nozzle and detected with a HeNe laser. The scattered light signals from single particles are used to externally trigger the excimer laser to fire and desorb and ionize species from each particle. Interestingly, detection of small particles with this technique is limited by optical detection not the mass spectrometer. Both lasers are aligned slightly offset to allow for the small time period between optical detection and arrival of the LDI pulse. The excimer laser is focused to a spot  $200\ \mu\text{m} \times 270\ \mu\text{m}$ , energies between 140 and  $340\ \mu\text{J}$  are applied with a pulse length of 13 ns, which corresponds to power densities between  $23$  and  $60 \times 10^6\ \text{W cm}^{-2}$ . The resulting ions are analyzed by acquiring either positive or negative spectra with a linear TOFMS.

With this experimental setup, monodisperse aerosols were analyzed allowing for instrumental characterization. Time-of-flight mass spectra were reported for both organic and inorganic particles. The first on-line single particle mass spectrum utilizing a TOFMS is shown in Figure 12. Cations such as  $\text{Na}^+$ ,  $\text{K}^+$ , and  $\text{NH}_4^+$  are observed as well as cluster ions including  $\text{NaKCl}^+$  and  $\text{K}_3\text{Cl}_2^+$ . It was found that ion currents varied from particle to particle while analyzing these monodisperse aerosols. This was attributed to the different positions of each particle inside the focused excimer laser beam allowing for differences in absorbed power densities and therefore differing ionization efficiencies. Also, time shifts associated with the same  $m/z$  were seen from particle to particle, again caused by differing locations in the source and/or laser beam during ionization. Second, relatively poor resolution, 90 at  $m/z$  39, was observed and is evident in Figure 12. This was due to a linear TOFMS, which inherently has lower energy resolution. During particle ionization, ions are created with initial velocity vectors both toward and away from the detector that lead to a much wider kinetic energy distribution than observed off surfaces and in gas-phase mass spectra. Although this first on-line aerosol TOFMS had several limitations, it illustrated that the general design utilizing LDI coupled with TOFMS could be applied to single particle analysis.

Since its inception, this general design has been improved as is illustrated in the following sections.

#### 4. Johnston and Wexler, RSMS (1994)

The instrument developed by Johnston and Murphy is the same design utilized by Johnston and Wexler with slight variations. In this modern version, used for rapid single-particle mass spectrometry (RSMS),<sup>137</sup> particles are introduced through a nozzle<sup>138</sup> into a differentially pumped region. Two skimmers are then used to allow for particle collimation as well as the necessary pressure drop for MS analysis. Next, each particle is optically detected with a helium-cadmium or helium-neon laser. No particle size information is obtained from this light scattering intensity due to high uncertainty (see Sections IV-B-5 and 6). This scattered light is detected by a PMT and subsequently an excimer laser is triggered for LDI of a single particle. These lasers are offset in such a manner as to maximize the particle hit rate. The excimer laser operates at 248 nm focused to a spot size of  $250\ \mu\text{m} \times 200\ \mu\text{m}$  and supplies between 0.1 and 5 mJ of energy with a pulse width of 2.5 ns. This corresponds to power densities between  $1 \times 10^8$  and  $2 \times 10^9\ \text{W cm}^{-2}$ , which allows for analysis of many compounds. A definite improvement in this design was the application of a reflectron in the TOF region. With this addition, resolution was improved to allow for baseline separation up to  $m/z$  300. Recently, RSMS-II has been developed<sup>139,140</sup> based on an earlier design<sup>141,142</sup> coupling a new particle inlet<sup>143</sup> with a TOFMS. This design allows for composition information from ultrafine particles, down to 12 nm,<sup>139</sup> which are too small for optical detection.

Johnston and Wexler have concentrated on laboratory-based studies utilizing synthetic aerosols. First, it was shown that ionic species such as  $\text{Fe}^{3+}$ ,  $\text{Na}^+$ ,  $\text{NO}_3^-$ , and  $\text{SO}_4^{2-}$  could be quantified in single glycerol microdroplets.<sup>144</sup> The liquid solvent allows for a reproducible matrix and particle morphology. Therefore, LDI, a technique not necessarily synonymous with quantification, can be used to quantitate ionic compounds in aerosol droplets. Next, a detailed study on matrix-assisted laser desorption/ionization (MALDI) was accomplished studying both a liquid, 3-nitrobenzyl alcohol (NBA), and a solid, 2,5-dihydroxybenzoic acid (DHB), matrix.<sup>145</sup> It was shown that as the analyte-to-matrix mole ratio increased, the analyte signal increased up to a point. In either case, solid or liquid, the signal increases until a monolayer of analyte covers the particle surface and then levels off. Also, quenching effects were observed when multiple analytes were present in single particles competing for surface adsorption sites.

Sulfur-containing and chromium-containing particles were synthesized and studied. In the case of sulfur, particles including sodium and ammonium sulfate and sulfite were studied.<sup>146</sup> High-mass cluster ions such as  $\text{NaSO}_4 \cdot \text{Na}_2\text{SO}_4^-$  ( $m/z$  261) in sodium sulfate particles and  $\text{CH}_3\text{SO}_3 \cdot (\text{SO}_4)_2^-$  ( $m/z$  287) in methanesulfonic acid (MSA) particles are more frequent and more intense in  $1.5\ \mu\text{m}$  particles than in  $3\ \mu\text{m}$  particles. Interestingly, this illustrates increased particle size having an inverse effect on MS



signal intensity. It was also shown that chromium oxide clusters up to  $\text{Cr}_2\text{O}_6^-$  are produced in  $3.7\ \mu\text{m}$  particles while clusters up to  $\text{Cr}_4\text{O}_{12}^-$  are apparent in larger  $9.5\ \mu\text{m}$  chromium nitrate particles.<sup>147</sup>

Studies have been done involving multicomponent crystallization as well as monitoring surface and total composition of aerosols. The crystallization experiment and thermodynamic analysis show that particles dried from various salt solutions possess surface compositions identical to the eutonic composition.<sup>148</sup> This leads to an enrichment of the minor component in the surface layer. Moreover, the products of a heterogeneous reaction, NaCl particles with gaseous ammonia and nitric acid, were monitored at low and high laser powers.<sup>149</sup> At low powers near the ionization threshold, approximately  $8 \times 10^7\ \text{W cm}^{-2}$ , only material near the surface was ionized, while at higher power densities, about  $5 \times 10^8\ \text{W cm}^{-2}$ , the entire aerosol is ablated. Results show that mass spectra were independent of deposited ammonium nitrate for low laser powers illustrating only a nitrate-rich surface layer. At higher powers, relative increases in the ammonium nitrate signal with increasing surface layers were observed. However, ammonium nitrate could not be quantitated due to particle-to-particle variations.

Ultrafine particles<sup>139,140</sup> and humidity effects<sup>150,151</sup> were studied on laboratory generated aerosols. Particles between 12 and 150 nm were analyzed using RSMS-II by firing the excimer laser at a constant frequency. It was found that free electrons rather than atomic or molecular ions dominated negative ion spectra. Also, positive ion spectra obtained are similar to those of larger micron size particles as ion signal intensity decreases only slightly with particle size. Next, laboratory-generated particles were observed at relative humidities above and below the respective deliquescence point for homogeneous particles<sup>150</sup> and multicomponent aerosols.<sup>151</sup> The deliquescence point represents a certain relative humidity where a dry particle becomes an aqueous droplet. This concept was studied, as negative ion spectra were reported for sodium chloride, Figure 13, ammonium nitrate and sulfate. Figure 13 illustrates an abrupt change in the NaCl negative ion mass spectra, obtained with 193 nm radiation, between a wet and dry particle over a narrow humidity range. The deliquescence point of sodium chloride particles is at a relative humidity of 75%. Therefore, Figures 13a and 13b represent the spectra of droplets showing prominent peaks for  $\text{Cl}^-$  ( $m/z$  35,37) and  $(\text{NaCl})\text{Cl}^-$  ( $m/z$  93–97). In comparison, Figures 13d and 13e represent spectra for dry particles with more intense signals as well as new peaks. Interestingly, ammonium nitrate undergoes a more gradual spectral transition with increasing humidity and ammonium sulfate undergoes very little change. The multicomponent aerosol study illustrated that the chemical composition can change as relative humidity is raised above the deliquescence point. In either case of homogeneous or multicomponent aerosols, water can arise from either adsorption at atmospheric pressure or condensation during introduction through the nozzle. The latter depends on nozzle geometry<sup>152</sup> and

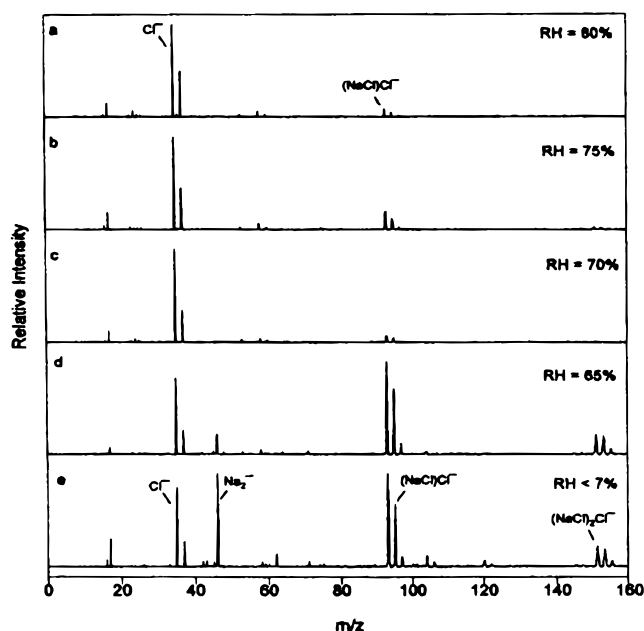


**Figure 13.** Negative ion mass spectra of sodium chloride particles collected at different relative humidities. Each spectrum represents an average of 10 particles. (Reproduced with permission from ref 150. Copyright 1998 Elsevier Science.)

was determined not to be a major source of particle phase water in these studies.

Although each application involved laboratory generated aerosols, all results have relevance to ambient aerosols. When studying atmospheric particles, it is essential to understand how different matrixes, relative humidities, and multiple components affect not only aerosols but also the instrumental responses to each of these factors. Therefore, these issues are important as they emphasize the difficulty in quantitation of ambient aerosols.

### 5. Murphy, PALMS (1994)

Murphy described another time-of-flight instrument,<sup>153,154</sup> particle analysis by laser mass spectrometry (PALMS), that consists of a differentially pumped inlet containing a capillary nozzle and two orifices. After particles traverse the inlet into the source region, each particle is detected optically by a HeNe, or a frequency doubled Nd:YAG, laser that is used to obtain qualitative size information as well as fire the desorption/ionization excimer laser. An avalanche photodiode, or more recently a photomultiplier tube, collects scattered light. Unfortunately, particles may travel in different areas within the scattering laser beam. This accounts for varying pulse heights for monodisperse aerosols as well as undersizing particles that travel on the edges of the beam. Particle shape and refractive index also affect scattered light intensity during ambient sampling. Nevertheless, this technique is used for obtaining coarse estimates of particle size. After ionization, the ions are mass analyzed by a TOFMS which first utilized post source pulse focusing<sup>154</sup> and later a reflectron<sup>155</sup> to improve mass resolution. A microchannel plate (MCP) is used as an ion detector.

The wavelength choice for the desorption/ionization laser was studied. It was shown that ion formation

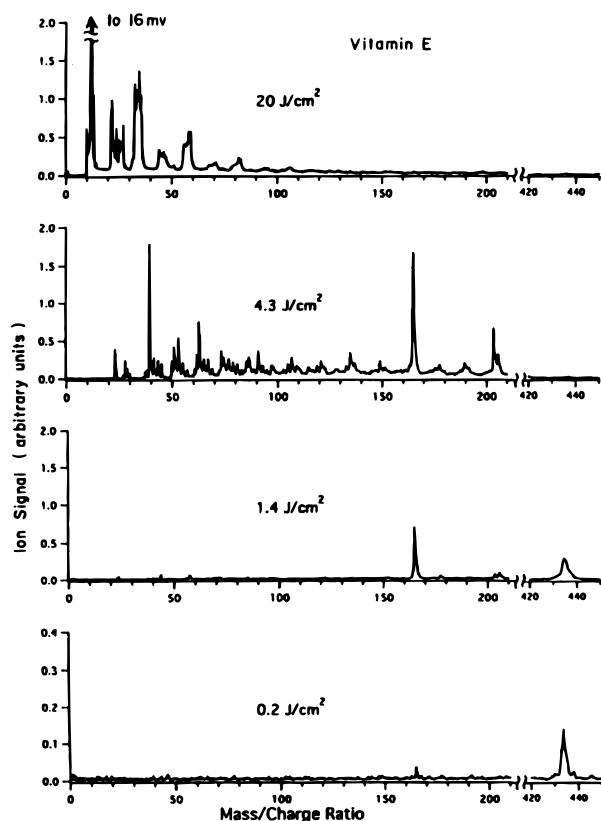


**Figure 14.** Spectra of single vitamin E particles illustrating the dependence of ion yield and fragmentation pattern on laser energy. Just above laser threshold, only the parent ion is detected, while at 100 times the energy the parent peak has disappeared and elemental carbon (off scale) is the largest peak. Note: not all compounds yield molecular ion signals at threshold energies. (Reproduced with permission from ref 154. Copyright 1995 Elsevier Science.)

thresholds decrease with laser wavelength. The  $\text{CO}_2$ ,  $10.6\text{ }\mu\text{m}$ , and excimer lasers, at 308 and 248 nm, were studied.<sup>60</sup> It was found that  $3 \times 10^9\text{ W cm}^{-2}$  was the threshold for partial ionization from the  $\text{CO}_2$  laser while about  $200 \times 10^6\text{ W cm}^{-2}$  from the excimer laser at 308 nm allowed for observation of molecular mass spectra. As the wavelength decreases into the vacuum-ultraviolet, even lower ionization thresholds are observed because nearly all substances have higher absorption coefficients at these lower wavelengths. The excimer laser was then utilized at 248, 193, and 157 nm.<sup>61</sup> At 248 and 193 nm, ionization thresholds depend on such variables as particle size and absorption coefficient, but it was shown that 157 nm radiation lessened the variation in thresholds for different compounds. Again, this is due to much higher absorption coefficients. It was also shown that thresholds for negative ion formation were greater than that of positive ions at all wavelengths. Interestingly, with each wavelength and increasing energy applied, there are different mass spectral characteristics. This is illustrated at 248 nm in Figure 14.<sup>154</sup> Here, Vitamin E is analyzed at various laser fluences. At its threshold of  $0.2\text{ J cm}^{-2}$ , only the molecular ion is detected. Then, as the laser power is increased, more and more fragmentation occurs until only low mass fragments are obtained. In general, due to relatively high ion thresholds and extensive fragmentation, lower wavelengths such as 157 nm are

more advantageous. However, the disadvantages of using 157 nm radiation are too limiting for it to be applied today, as they include lower available energy compared to higher wavelengths and the strong absorption by water vapor and oxygen. After these studies, Murphy has utilized either 248 or 193 nm radiation for recent applications.

Unlike Johnston and Wexler, Murphy mainly focuses on field measurements. First, aerosol characteristics were studied at Idaho Hill, CO, by taking size measurements<sup>156</sup> and both positive<sup>157</sup> and negative<sup>158</sup> mass spectra. PALMS detected alkali metals, iron, organics, and ammonium in positive ion configuration. Correlations between chemical composition and particle size were determined. Examples include, organics being the main contributor in the accumulation mode and metals, such as iron, occurring dominantly in coarse mode particles. In negative ion polarity, the most common peaks were sulfate, nitrate,  $\text{O}^-$ ,  $\text{OH}^-$ , and organics. It was observed that nitrate was correlated with particles larger than  $0.7\text{ }\mu\text{m}$  while sulfate was more common in smaller particles. Marine aerosols were studied next at Cape Grim, Tasmania. Bromine, iodine, and chlorine were observed in aerosols from this area.<sup>159</sup> Chlorine was most prominent, while bromine was present in amounts close to the seawater mole fraction and iodine was greatly enriched compared to its natural seawater abundance. Furthermore, aerosols containing sulfate, metals, and  $\text{NO}^+$  were examined.<sup>155</sup> Sulfate was mixed with sea salt particles while  $\text{NO}^+$  was associated with Mg, Ca, and Sr. Finally, internally mixed organic material was observed with single sea salt particles.<sup>160</sup> The detected organics were assigned to two possible sources: those originating from bursting bubbles on the ocean surface or from oxidation of gas-phase organics emitted from the ocean. These aerosols were again analyzed, but in terms of sea salts influence on radiative properties.<sup>161</sup> Intermediate sizes between  $0.08$  and  $1\text{ }\mu\text{m}$  are the most important for aerosol radiative effects in the marine boundary layer due to their efficient light scattering characteristics as well as their role as cloud condensation nuclei. It was shown in the marine boundary layer most aerosols larger than  $0.13\text{ }\mu\text{m}$  contain sea salt, contradicting earlier belief that particles below  $1\text{ }\mu\text{m}$  were non-sea-salt-sulfate. Moreover, these aerosols were determined to be responsible for the majority of light scattering.

PALMS was recently deployed for upper tropospheric and lower stratospheric particle analysis. Before field measurements were taken, laboratory-generated sulfuric acid particles were studied to simulate stratospheric aerosols.<sup>162</sup> Then, in 1998, the instrument was mounted in the nose of a high altitude research plane and both positive and negative spectra were taken in the upper troposphere and stratosphere.<sup>163</sup> Representative spectra from three different particles are shown in Figure 15. Spectrum A represents common upper tropospheric particles containing organic, halogen, and sulfate peaks in a negative ion spectrum. Spectra B and C represent common stratospheric particles that contain sulfate in negative polarity and metals such as magnesium

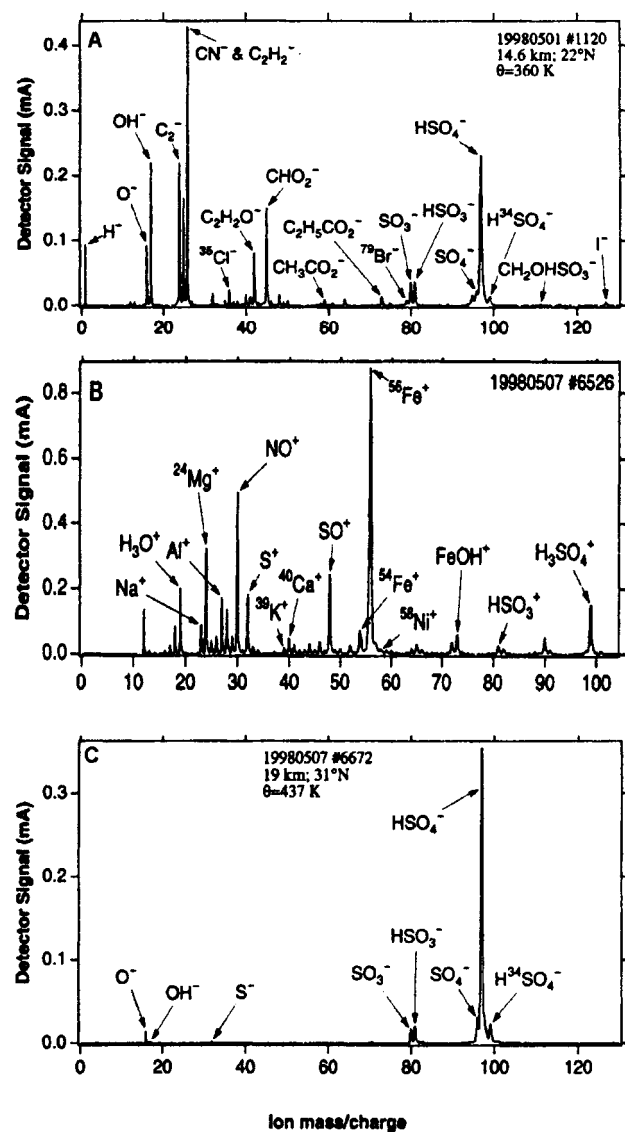


**Figure 15.** Representative spectra from the upper troposphere (A) and the lower stratosphere (B and C). A represents a common negative ion mass spectrum of an upper tropospheric particle containing organics, halogens, and sulfate. B and C represent positive and negative ion mass spectra, respectively, from the stratosphere containing mainly sulfate with other constituents such as iron. (Reproduced and modified with permission from ref 163. Copyright 1998 American Association for the Advancement of Science.)

and iron in positive ion configuration. Interestingly, two types of evidence indicate that iron in the stratosphere is from a meteoritic source. First, iron peaks were more common in the stratosphere than the upper troposphere, suggesting that there must be a high altitude iron source. Second, the iron containing particles also contained other metals such as sodium, aluminum, potassium, and nickel in proportions consistent with material from meteorites.

#### 6. Prather, ATOFMS (1994)

Aerosol time-of-flight mass spectrometry has the ability to precisely size individual particles in a polydisperse aerosol as well as obtain chemical composition data on single particles. First, a laboratory instrument was described.<sup>164–166</sup> Particles are

introduced through a nozzle and collimated through three skimmers. After passing through this differentially pumped region, particles encounter two continuous wave lasers, oriented at right angles, which are used in conjunction with a timing circuit for determination of particle size. A particle passes through the first light scattering Ar<sup>+</sup> laser and is detected by a PMT. This signal starts a timing circuit. Next, the particle travels a known distance and is detected by light scattering of another continuous wave laser, earlier a HeNe and more recently an Ar<sup>+</sup> laser. This PMT signal stops the timing circuit. The recorded time is directly related to the aerodynamic diameter of a particle and with appropriate calibration can be used to determine particle size. Unlike sizing techniques utilizing light scattering intensity measurements, this sizing method does not depend on particle trajectory through the laser beams. Hence, this design accounts for any velocity spread and constitutes the most precise and reproducible modern sizing technique incorporated with single particle mass spectrometry. At this point, the particle has three times the distance to travel from the second continuous wave laser to the source region of the mass spectrometer than between the two scattering lasers. Therefore, the timing circuit counts down at one-third the rate. The circuit then externally triggers either a Nd:YAG, at 266 nm, or a CO<sub>2</sub> laser while also accounting for the amount of time needed for the pulse to reach the middle of the source region. Here, a single particle is desorbed and ionized from this triggered laser pulse. The ions are analyzed in a reflectron time-of-flight mass spectrometer and detected using a MCP. This laboratory-based instrument is still limited by its single polarity. It is able to acquire only a positive or negative mass spectrum for individual particles, similar to earlier TOFMS aerosol mass spectrometers.

More recently, two field transportable instruments were developed and described,<sup>75</sup> overcoming the single polarity limitation. These instruments, schematically illustrated in Figure 5, incorporate a similar inlet and aerodynamic particle sizing region along with a dual polarity reflectron time-of-flight-mass spectrometer. The inlet consists of a nozzle and two skimmers, while the sizing region, most recently, utilizes diode pumped Nd:YAG lasers.<sup>167</sup> After particle ionization, cations and anions are accelerated in opposite directions. In both cases ions travel through holes in the center of both detectors, most recently MCPs, which are mounted directly outside the ion source region and are floated at high voltages to maintain a field free region. Both polarities utilize reflectrons allowing for ions to reverse direction and be detected by the MCPs, which are mounted just outside of the source region. Overall, this design allows for not only precise size measurement, but also the ability to travel and take measurements in the field while simultaneously acquiring both positive and negative spectra from individual particles.

Applications consist of both laboratory-based studies and ambient aerosol measurements. First, single particle laboratory experiments have been reported. A comparison of particle sizing techniques, utilizing



the dual beam aerodynamic sizing technique versus light scattering signal intensity has been explored.<sup>168</sup> It was determined that standard deviations in particle size were greater than 50% when utilizing light scattering intensity from single particles while deviations from 1 to 11% were found with the aerodynamic sizing technique. The large deviations with the former are attributed to particle size, shape, refractive index, and differing trajectories through the beam profiles. On the contrary, utilizing aerodynamic sizing with signals from two continuous wave lasers with a timing circuit allows for much more precise sizing of single particles. Next, two-step laser desorption/ionization (L2MS), a softer ionization process, was applied to single organic particles to allow for molecular ion determination.<sup>169</sup> Cigarette and wood smoke particles were first desorbed by a CO<sub>2</sub> laser, with a power density of approximately  $1 \times 10^7$  W cm<sup>-2</sup>, and subsequently ionized by a 266 nm Nd:YAG pulse at a lower power density, about  $5 \times 10^6$  W cm<sup>-2</sup>. It was shown that PAH molecular ions can be identified in this manner, while PAH spectra obtained by conventional one step LDI are usually dominated by low mass fragments.

Other laboratory experiments include observation of particles from vehicular exhaust<sup>170</sup> and albuterol-metered dose inhalers.<sup>171</sup> Particles were sampled directly from numerous automobiles and analyzed using ATOFMS.<sup>170</sup> A qualitative correlation was found between particle size and composition. Particles less than 1  $\mu$ m were found to contain mainly organics, while inorganic species were dominant in the coarse particles greater than 1  $\mu$ m. Interestingly, substances such as lead, cerium, platinum and molybdenum were observed. This study illustrates the possible use of ATOFMS as an on-line vehicular emission aerosol monitor. Next, a bioanalytical study was reported on the observation of albuterol particles from a metered dose inhaler.<sup>171</sup> Typically, these drugs are characterized with off-line bulk analytical techniques. The ATOFMS study shows that on-line single particle mass spectrometry can be utilized for chemical composition determination of single particles in various drugs delivered to the body through use of aerosol inhalation devices. The example shown in Figure 16 illustrates positive mass spectra at high and low laser powers. Spectra obtained at lower laser powers contain signals from the protonated and deprotonated albuterol parent ion, while higher laser power spectra show peaks from fragmentation.

Ambient measurements have also been made with ATOFMS.<sup>172</sup> Single particle mass spectra were reported and grouped into appropriate classifications such as inorganic, soil, and sea salt, as well as organic, ammonium, sulfate, and nitrate containing particles. Size distributions for each particle type were compared with one another and to the total size distributions.<sup>173</sup> This study illustrates a definite particle size and composition correlation associated with approximately 1  $\mu$ m. Coarse mode inorganic particles are found to be mainly greater than 1  $\mu$ m while organic containing particles are found to be mainly less than 1  $\mu$ m. Ambient 4th of July fireworks particles were monitored.<sup>174</sup> This demonstrated the

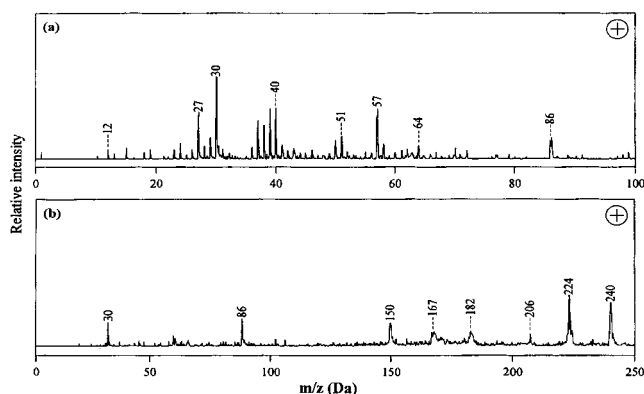


**Figure 16.** Positive LD mass spectra of single albuterol particles from a metered dose inhaler aerosol obtained at both high (a) and low (b) laser powers. High laser power corresponded to  $10^9$ – $10^{10}$  W cm<sup>-2</sup> while lower laser power corresponded to  $10^6$ – $10^7$  W cm<sup>-2</sup>. This shows that much less fragmentation occurs with lower energy. (Reproduced with permission from ref 171. Copyright 1998 Elsevier Science.)

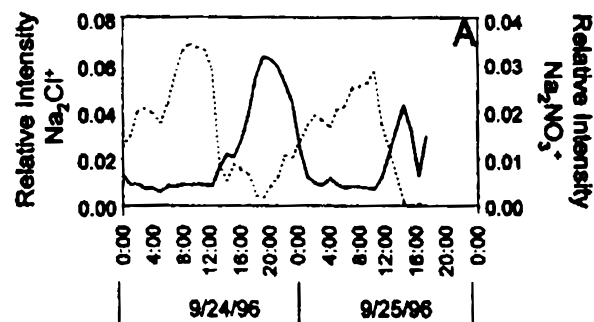
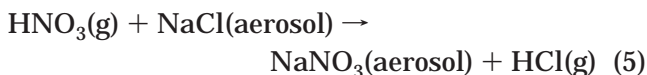


**Figure 17.** This figure represents 1 h average peak areas of chloride and nitrate markers, Na<sub>2</sub>Cl<sup>+</sup> and Na<sub>2</sub>NO<sub>3</sub><sup>+</sup>, respectively, over approximately a 2-day time period. Solid and dashed curves represent the average intensity of chloride and nitrate (or their respective markers) in sampled particles. (Reproduced with permission from ref 179. Copyright 1998 American Association for the Advancement of Science.)

ability to monitor a specific aerosol type, or source, in ambient particles on a real time basis. Observations were also made regarding single particles during winter rainstorms.<sup>175</sup> It was shown that particle scavenging occurs and that sea salt particles, mainly greater than 1  $\mu$ m, represent relatively more of the atmospheric particulate matter during winter rainstorms in Riverside, CA, than on clear days. Most recently, a heterogeneous chemical reaction involving the atmospheric replacement of chloride with NO<sub>x</sub> species in sea salt particles,<sup>176–178</sup> such as eq 5, was observed in Long Beach, CA.<sup>179</sup>



Sea salt particles were sampled by ATOFMS over a 2-day period. The relative peak areas of the chloride and nitrate marker ions, Na<sub>2</sub>Cl<sup>+</sup> and Na<sub>2</sub>NO<sub>3</sub><sup>+</sup>, were determined and the average plotted over time in 1-h periods. (See Figure 17) A diurnal variation was found to exist between these markers illustrating the ambient occurrence of reactions such as eq 5. Therefore, this study confirms that heterogeneous chem-

istry can be observed directly in the atmosphere in real time using single particle mass spectrometry.

### 7. Ramsey and Whitten (1994)

Ramsey and Whitten's real time single particle MS design is different from others as it utilizes an ion trap mass spectrometer.<sup>71</sup> This commercial instrument (Finnigan MAT, San Jose, CA, Model 800 ion trap detector) consists of two end cap electrodes and a ring electrode. Because of this unconventional application, the ITMS was specifically modified to allow for particle introduction and laser accessibility. This instrument along with the more current inlet system, analogous to Prather's, is shown in Figure 4. Before this inlet, a particle hopper<sup>180</sup> and then a solenoid<sup>181</sup> were used for introduction of aerosols into the ion trap. Particle levitation was utilized<sup>182,183</sup> as particle size could be estimated by observation through a telescope. Recently, a new inlet and sizing region consisting of a converging nozzle, two skimmers, two continuous wave Ar<sup>+</sup> lasers associated with photomultiplier tubes and a timing circuit is being utilized.<sup>184</sup> As mentioned earlier, this technique allows for precise particle size determination as well as an external trigger for the DI laser. After ionization, the ion trap mass spectrometer can analyze species from single particles. After a particle is ablated with either a Nd:YAG at 532 nm or an excimer laser at 308 nm, the resulting ions are confined to the ion trap. Subsequently, the rf voltage on the ring electrode can be ramped to eject and detect the ions sequentially for acquisition of a mass spectrum or a single ion,  $m/z$ , can be mass selected while ejecting all other ions. This single  $m/z$  can then be "tickled" by applying a rf voltage to the end cap electrode, causing collisional dissociation with the buffer gas. Subsequently, the ring rf voltage is ramped to mass analyze the fragment ions. This technique, known as MS/MS is very powerful for the determination of organic species in single particles and is illustrated by Ramsey and Whitten's applications.

Similar to Johnston and Wexler, Ramsey and Whitten have worked exclusively on laboratory-based studies. First, positive ion mass spectra were reported from tetraphenylammonium chloride and tetraphenylphosphonium bromide (TPPB) adsorbed on silicon carbide particles and a negative ion mass spectrum was obtained from 2,4,6-trinitrotoluene.<sup>180</sup> Second, positive spectra were obtained from levitated single microparticles of CuO and SiC coated with TPPB.<sup>182</sup> Next, examples of MS/MS were illustrated. Isolation of the major fragment of TPPB,  $\text{Ph}_4\text{P}^+$  shown in Figure 18a, was collisionally dissociated and mass analyzed to obtain the fragment ion mass spectrum shown in Figure 18b.<sup>71</sup> In Figure 18a, the spectrum shows many fragments, inorganic peaks, along with the parent molecular ion. Figure 18b illustrates the fragmentation pattern from 532 nm Nd:YAG radiation associated specifically with  $m/z$  339, which corresponds to the loss of one, two, and three phenyl rings. This example represents the type of information obtained from MS/MS and the importance of this technique for organic analysis. With

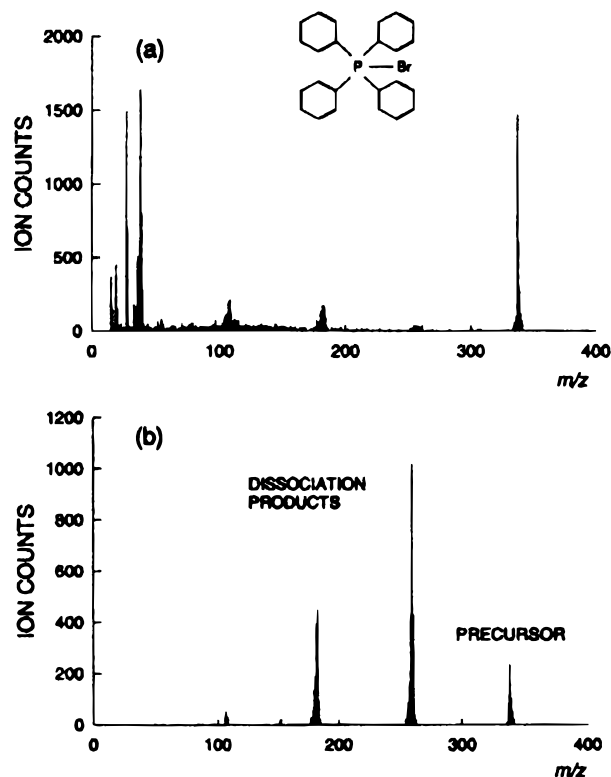


**Figure 18.** Demonstration of MS/MS organic analysis. Here, TPPB is condensed onto a SiC particle and mass analyzed by ITMS. Part a illustrates the primary mass spectrum and b represents the mass spectrum of the parent ion,  $m/z$  339, after collision induced dissociation. (Reproduced with permission from ref 71. Copyright 1996 John Wiley & Sons.)

laser desorption/ionization, organic molecules mainly lead to highly complex fragmented spectra. Unknown parent ions and/or fragment ions can be isolated and analyzed by MS/MS to obtain further information leading to identification of organic molecules and/or functional groups. Furthermore, it was shown that the degree of fragmentation is inversely related to the total number of ions produced in the ITMS.<sup>181</sup> Another MS/MS experiment utilized tributyl phosphate and bis(2-ethylexyl) phosphate on silicon carbide and kaolin microparticles to obtain structural information regarding molecular species in microparticles.<sup>184</sup>

For newer studies, an excimer laser was utilized at 308 nm. Most recently, individual bacteria particles, uranium and uranium oxide particles, and diesel exhaust were analyzed. First, mass spectra of freeze-dried bacteria including *Bacillus subtilis* and *Escherichia coli*, *E. coli*, strain K-12 were reported.<sup>185</sup> Figure 19 illustrates a negative ion mass spectrum from a single cell of *B. subtilis*, while the arrows correspond to mass fragments identified through MS/MS analysis. Because  $m/z$  79 loses 16 mass units, or oxygen, and  $m/z$  97 fragments into  $m/z$  79, losing 18 mass units or oxygen with two protons, it is probable that  $m/z$  79 is  $\text{PO}_3^-$  and  $m/z$  97 is  $\text{H}_2\text{PO}_4^-$ . These assignments allow for determination of higher mass ions, as  $m/z$  97 predominates in the MS/MS spectra of  $m/z$  181, 241, and 261. Therefore, these ions most likely represent organophosphate or pyrophosphate ions. This example again illustrates the

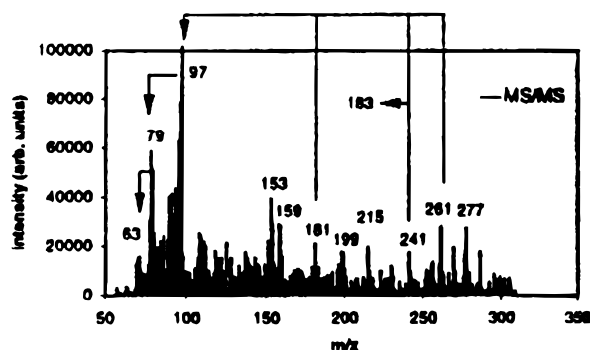


**Figure 19.** A negative ion mass spectrum from a single cell of *Bacillus subtilis*. The arrows correspond to fragmentation that results after collision-induced dissociation of the selected ions in other experiments. (Reproduced with permission from ref 185. Copyright 1997 Elsevier Science.)

importance of MS/MS for single particle analysis. Next, uranium was analyzed in several matrixes with 7-amino-1,3-naphthalenedisulfonic acid (ANDSA) being the most favorable.<sup>186</sup> The single particle detection limit for uranium, in the forms  $\text{UO}_2^+$  at  $m/z$  270 and  $\text{UO}^{2+}$  at  $m/z$  127, was determined in ANDSA to be in the subattogram range. As mentioned earlier, reactions can take place during the desorption/ionization process. Interestingly, due to the length of time ions are present in the source region of an ITMS, reactions with the background gases are possible. Unlike TOFMS, in which ions spend approximately a microsecond in the source region, ions within an ITMS are present for milliseconds in the mass spectrometer before detection. Therefore, some ions are able to react with background gases depending upon their decay rates. This was examined by comparing fragments associated with TOF mass spectra and ion trap mass spectra. It was found that in TOF spectra, peaks associated with  $\text{U}^+$ ,  $\text{UO}^+$ , and  $\text{UO}_2^+$  were the dominant ions. This means that these ions were formed in the DI process while the main ions detected by ITMS were created after DI by reaction with  $4 \times 10^{-5}$  Torr of air pressure. This was experimentally determined by measuring decay constants for each of these components. It was discovered that both ions detected by ITMS had relatively long decay rates. Moreover, this was illustrated with MS/MS by isolating  $m/z$  127 and varying the trap times from 5.7 to 255.7 ms. As time increased, the amount of  $\text{UO}_2^+$  increased illustrating the formation of this component by reaction with air over time. These results show that comparison of LDI ion trap mass spectra with TOF mass spectra may not be appropriate due to possible reaction of ions within the ion trap that form species not found in TOF spectra. Finally, individual diesel engine exhaust particles were collected and analyzed.<sup>187</sup> Spectra were obtained from cold, warm, and hot engines. Averaged spectra were compared with each other and spectra from nebulized diesel fuel and engine oil. Numerous PAHs including indene, phenanthrene, and acenaphthylene were positively identified through MS/MS analysis.

#### 8. Reents (1994)

Reents developed an on-line instrument that is based on a different premise from others described

so far. Small particles, approximately 10–20 nm and greater, associated with the manufacturing of semiconductor devices are of interest. Therefore, light scattering cannot be utilized because of the size limitation associated with optical detection. Aerosols are introduced through a capillary nozzle and two skimmers into the source region of a linear TOFMS where a pulsed excimer laser is fired between 10 and 30 Hz.<sup>141</sup> With this design, particles between approximately 0.02–10  $\mu\text{m}$  can be analyzed allowing for much smaller particle size analysis than with light scattering techniques. The excimer laser is focused to a rectangular spot size of 0.08 cm  $\times$  0.3 cm, operated at 308 nm with a 40 ns pulse width, allowing for a power density of approximately  $1.7 \times 10^8 \text{ W cm}^{-2}$ . Although smaller particles can be analyzed, a much lower particle hit rate is found compared to other instruments that utilize optical detection.<sup>141,142</sup> This is due to the random firing of the excimer laser as well as lower transmission efficiencies due to greater divergence of smaller particles. It was shown that ion signal intensity versus particle size was linear under 1  $\mu\text{m}$ .<sup>141</sup> Spectra were obtained from species such as ammonium sulfate and silica,<sup>141,142</sup> and mass resolution was reported to increase with decreasing particle size.<sup>142</sup> This design illustrates that on-line particle MS instruments can use LDI to analyze aerosols smaller than optical detection currently allows.

#### 9. Russell and Murray (1994)

Uniquely, TOFMS was utilized with matrix-assisted laser desorption ionization and coupled with high-performance liquid chromatography (HPLC).<sup>188</sup> Briefly, MALDI utilizes a matrix to help in the ionization process of large biomolecules. The solvents are evaporated leaving the matrix and analyte in a solid form. Subsequently, a pulsed laser is absorbed by the matrix, causing surface ablation and ionization of the intact biomolecule. This allows for mass spectral analysis of the parent molecule. This technique has been coupled with HPLC by combining the effluent with an appropriate matrix in a mixing tee, nebulizing the sample into a vacuum chamber and a drying tube, 25 cm long, 4 mm inner diameter, heated to 300  $^\circ\text{C}$ , is used for skimming along with desolvating the aerosol before entering the source region where DI is accomplished on a cloud of particles by a Nd:YAG at 355 nm.<sup>189</sup> This system can also be disconnected from the HPLC, allowing for direct introduction of an analyte/matrix solution by nebulization into the mass spectrometer. The resulting ions are mass analyzed by a linear TOFMS, or more recently a reflectron system<sup>190</sup> for improved resolution, and detected by a MCP.

Different aspects of MALDI have been reported. First, a separation of peptides and proteins, bradykinin (MW = 1060), gramicidin S (MW = 1142), and myoglobin (MW = 16 951, was accomplished by HPLC and detected, after mixing with the  $\alpha$ -cyano-4-hydroxycinnamic acid matrix, by TOFMS.<sup>188</sup> Next, bovine insulin was analyzed in numerous matrixes including 4-nitroaniline and 2-cyano-4-nitroaniline.<sup>191</sup> Interestingly, the optimum matrix-to-analyte ratio



was determined to be the opposite compared to surface MALDI. In aerosol MALDI, the optimum amount of analyte corresponds with the maximum amount that can be dissolved in solution. Therefore, the lowest matrix-to-analyte ratio possible is desired. Experimentally, this corresponded to 50:1 compared with typical surface MALDI ratios between 100 and 50000:1. Moreover, ion yield was determined to be greatest at lowest matrix-to-analyte ratios<sup>192</sup> and solvent effects on MALDI ion signals were studied.<sup>193</sup> Finally, a reflectron TOFMS was utilized allowing for resolution of over 300, which represented a 10-fold increase compared to the linear geometry, for peptides including angiotensin II and vitamin B<sub>12</sub>.<sup>190</sup> Even with this improvement, this technique has much lower mass resolution and higher detection limits than conventional MALDI and does not utilize particle sizing techniques of other on-line aerosol TOFMS instruments. However, introduction of MALDI to aerosol analysis was demonstrated, allowing for TOF mass spectral detection of biomolecules up to approximately 30 kDa.

#### 10. Spengler, Kaufmann, and Hinz, LAMPAS (1994)

Laser mass analysis of particles in the airborne state (LAMPAS) utilizes a differentially pumped particle beam generator consisting of a nozzle and two skimmers, a single HeNe laser and a PMT for particle detection, a nitrogen laser for DI, and a TOFMS and an MCP for ion detection.<sup>194,195</sup> PMT placement was studied by modeling the light scattering profile with Mie theory. It was determined that an angle of 45° was more efficient than 90° geometry utilized by other similar instruments.<sup>194</sup> Furthermore, the HeNe and DI lasers are offset by approximately 500–750  $\mu\text{m}$  and the signal from the continuous wave laser is used to trigger the ionization laser. Therefore, particle size information may be obtained from the duration of the scattering pulse from the HeNe laser or from the time delay between the two lasers if the particle is ablated. By varying the delay time between the detected scattered light pulse and the DI laser, different particle sizes can be analyzed. After ionization, mass analysis was first accomplished with a linear, and more recently with a reflectron, time-of-flight MS. In 1996, these authors reported the first dual polarity design.<sup>195</sup> After DI, positive ions are accelerated in one direction down an 1100 mm flight tube possessing PSPF to improve mass resolution, while negative ions are accelerated in the opposite direction down a 400 mm flight tube. In both tubes, MCPs are used as ion detectors. This design led to the first on-line positive and negative mass spectra for a single ambient particle. (See Figure 20) This particle is composed of soot as well as nitrate and sulfate. Moreover, 253 of these laboratory air particles were analyzed by Principal Component Analysis to identify certain classes of particles and their dominant chemical components.<sup>195</sup> Finally, a study utilizing delayed extraction applied to MALDI was accomplished illustrating a significant improvement in mass resolution of up to 1800.<sup>196</sup>

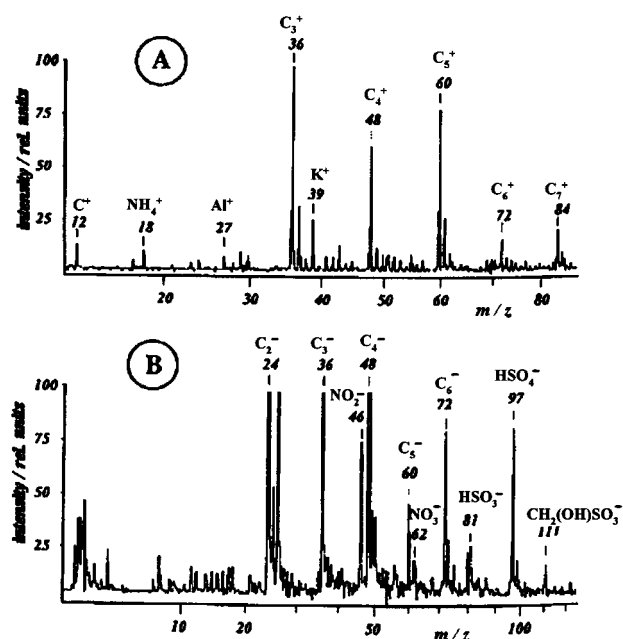


**Figure 20.** The first on-line positive (A) and negative (B) mass spectra simultaneously obtained. These ambient laboratory air particle mass spectra represent a soot particle containing both nitrate and sulfate. (Reproduced with permission from ref 195. Copyright 1996 Elsevier Science.)

#### C. Newer Members to the Aerosol MS Field

Recently, Marijnissen constructed an on-line single particle mass spectrometer based on his proposed earlier design.<sup>197,198</sup> These articles also include a detailed discussion and analysis of the theory behind different nozzle geometries and particle transmission along with detailed instrument characterization. Another single particle laboratory-based TOFMS utilizing LDI is an instrument developed by Whetten to analyze particles in the 1–10 nm size range.<sup>199</sup> There are also several on-line designs utilizing quadrupole mass spectrometers in conjunction with aerodynamic lenses<sup>44,45</sup> to create a narrow, low divergence particle beam. In one system, a thermal desorption particle beam mass spectrometer (TDPBMS) allows for mass analysis of ions created from particle impaction on a heated, V-shaped molybdenum foil.<sup>200</sup> This laboratory-based instrument constructed by Ziemann can quantify certain particulate organic components as well as monitor secondary organic aerosols formed during smog chamber reactions. In a second system, an aerosol mass spectrometer (AMS) has been developed by Jayne and co-workers that takes advantage of both surface/thermal ionization in conjunction with EI.<sup>201</sup> This instrument can obtain aerodynamic size as well as chemical composition information and has shown to be quantitative for laboratory generated NH<sub>4</sub>NO<sub>3</sub> particles less than 1  $\mu\text{m}$ . Third, a balloon based ion molecule reaction mass spectrometer (IMRMS) equipped with a vaporizer has been developed by Arnold et al. for determination of sulfuric acid content in stratospheric particulates.<sup>202</sup> More recently, aerodynamic lenses were used for particle introduction during their measurements within polar stratospheric cloud layers.<sup>203</sup> Finally, organic aerosol products of the reaction between O<sub>3</sub> and  $\alpha$ -pinene

were introduced into an atmospheric pressure chemical ionization mass spectrometer (APCI/MS) in which MS/MS experiments were done to identify specific species.<sup>204</sup> Undoubtedly, these newer members to the aerosol mass spectrometry community represent the first of many researchers who will join this exciting and rapidly developing field in the years to come.

## V. Discussion/Conclusions

The field of aerosol mass spectrometry has advanced substantially since its inception. Off-line analysis of filter samples utilizing LAMMS, SIMS, and ICPMS allowed for the understanding of many advantages and limitations of aerosol measurement techniques. Although many invaluable studies were conducted with these techniques, off-line analysis was, and to this day still is, greatly limited by filter sampling and possible alteration of the aerosol before analysis. However, some information is available exclusively from off-line instruments, such as depth profiling and the ability to obtain multiple mass spectra per particle. Off-line aerosol techniques will continue to be utilized and supply complementary information to newer on-line methods. Table 3 summarizes the development of this on-line field by including instrumentation utilized, as well as the major advancements each of the on-line aerosol mass spectrometry pioneers have contributed.

Instrument development has greatly improved the performance and general utility of on-line aerosol mass spectrometers. The surface ionization era most notably combined knowledge on inlet designs from earlier particle beam research with mass spectrometry allowing ambient aerosols to be introduced directly into the source region of a MS. This knowledge has been applied to nearly all modern on-line MS instruments. Most recently, the field utilizes continuous wave lasers for optical detection of individual particles, UV wavelength DI lasers or surface vaporization with EI for ionization and time-of-flight, ion trap, or quadrupole mass spectrometers. In addition, the use of a timing circuit and optical detection for aerodynamic sizing allows for precise size determination of aerosols. For many reasons, including visibility and climate change studies along with characterizing particles that pose the greatest health risk to humans, monitoring particle size as well as chemical composition will help gain insight into aerosol processes and dynamics. For example, from data obtained from aerosol mass spectrometers, a major difference in particle composition is observed at approximately 1  $\mu\text{m}$ . Although many instruments have observed this before, off-line as well as on-line mass spectrometers confirm this correlation. It has been shown that combustion and other organic particles are mainly found less than 1  $\mu\text{m}$  while less pathogenic particles such as sea salt and soil are found in particulates greater than 1  $\mu\text{m}$ . From data such as this, the future may hold another USEPA particulate standard for smaller particles (i.e.,  $\text{PM}_{1.0}$ ) in addition to the current standards of  $\text{PM}_{2.5}$  and  $\text{PM}_{10}$ .

Throughout this review, much on-line instrumentation has been discussed that encompasses slightly

different sample inlets, different particle sizing techniques utilizing different lasers, and different mass spectrometers. It is important to understand that each instrument has been developed for specific purposes. First, after the particles are introduced into the system via the particle beam inlet, each research group has decided whether particle size determination is vital to their experiments. In Johnston and Wexler's case, particle size information is not determined because of their specific laboratory applications. This has lead them to use a single continuous wave laser to detect particles and nearly instantaneously fire their excimer laser. In the case of Prather, who not only conducts laboratory studies but also field work, particle size determination is paramount. Here, a Nd:YAG DI laser is utilized, due to its better beam homogeneity compared with the excimer laser, along with two low power continuous wave lasers for precise aerodynamic sizing. Particle beam divergence affects this system more so than Johnston and Wexler's because of the longer distance the particle beam must traverse. Currently, this general instrumental arrangement for aerodynamic sizing is the only one that allows for the use of a Nd:YAG laser due to the longer time period needed to fire this type of laser. The systems developed by Sinha and Spengler, Kaufmann and Hinz are essentially a compromise as they can analyze monodisperse aerosols by varying the delay time between the detected scattered light signal and DI laser pulse. The tradeoff is they can only chemically analyze one size at a time. Therefore, each of these designs offers different choices of instrumentation that may be applied to specific or very broad types of applications. Second, after LDI either a TOF or an ion trap mass spectrometer have been utilized. Regarding TOFMS, reflectron instruments have shown to give much greater mass resolution than linear systems while dual polarity instruments obtain all chemical information from a single particle (see Sections IV-B-6 and 10).

Currently, there is difficulty in both speciating organics and quantitation with single particle analysis using LDI. Organic determination is difficult with today's techniques due to the high-energy, multiphoton ionization process from relatively long wavelengths used for DI. This results in extensive fragmentation, not allowing for identification of parent organic molecules. Fortunately, an ion trap can, in many cases, determine organic molecular ions and functional groups utilizing MS/MS. This is an invaluable technique that will definitely be explored to a greater extent. Another likely direction, is the move toward shorter wavelengths leading to softer ionization and therefore less organic fragmentation. In the future, after commercialization of on-line single particle mass spectrometers, one wavelength and applied energy may be accepted as a standard so information can be more accurately compared between laboratories. This may occur because fragmentation and mass spectral characteristics greatly depend on power density and ionization wavelength utilized. Therefore, applying standards, similar to the electron impact gas-phase mass spectrometry field

**Table 3. Pioneers of On-line Single Particle Mass Spectrometry, a Historical Summary**

Research Group & Instrument Acronym	Sizing Method	Ionization Method	Mass Spectrometer	Advancements	References
Davis	Ion signal intensity	Surface/thermal	Single focusing magnetic sector	Began the field of on-line single particle mass spectrometry.	51 112,113
Lassiter & Moen	None	Surface/thermal	Quadrupole	Introduced quadrupole to single particle mass spectrometry.	114
Myers & Fite (SIMP)	Ion signal intensity	Surface/thermal	Quadrupole	Introduced Ru oven to lower particle size detection limits and analyzed negative ions.	115,116
Stoffels (DIMS)	Ion signal intensity	Surface/thermal	Double focusing triple sector	Introduced modern particle inlet & improved MS isotope abundance sensitivity, applied at Hanford.	67, 117-123
Allen & Gould (CAART)	Ion signal intensity	Surface/thermal & EI	Quadrupole	Introduced the combination of surface vaporization and EI to single particle MS.	124
Sinha & Friedlander (PAMS)	Ion signal intensity	Surface/thermal & EI	Quadrupole/magnetic sector	Characterized instrumentation. Analyzed biological compounds, quantitated mass of NaCl particles.	125-132
Sinha	Aerodynamic sizing (Monodisperse)	LDI	Quadrupole/magnetic sector	Introduced LDI to single particle MS and developed instrument for acquisition of entire spectrum.	133-134
Marijnissen	Light scattering intensity	LDI	Time-of-Flight	Proposed on-line TOFMS.	135 197-198
Johnston & Murphy	None	LDI	Linear Time-of-Flight	Constructed first on-line aerosol TOFMS. Published first on-line single particle TOF mass spectrum	136
Johnston & Wexler (RSMS)	None	LDI	Linear then Reflectron Time-of-Flight	Conducted laboratory based studies on aerosols including quantitation of microdroplet species.	137-140, 144-152
Murphy (PALMS)	Light scattering intensity	LDI	PSPF then Reflectron Time-of-Flight	Fundamental laser studies & numerous field studies including stratospheric measurements.	60,61, 153-163
Prather (ATOFMS)	Aerodynamic sizing (Polydisperse)	LDI	Reflectron Time-of-Flight	Applied precise sizing method along with dual polarity TOFMS in a transportable instrument.	75, 164-175, 179
Ramsey & Whitten	Aerodynamic sizing (Polydisperse)	LDI	Ion Trap	First to construct single particle ITMS. Demonstrated MS/MS experiments on single particles.	71, 180-187
Reents	None	LDI	Linear Time-of-Flight	Developed instrument without optical detection able to analyze ultrafine particles.	141,142
Russell & Murray	None	LDI	Linear then Reflectron Time-of-Flight	First to couple on-line particle MS with HPLC. Main focus on aerosol MALDI.	188-193
Spengler, Kaufmann & Hinz (LAMPAS)	Aerodynamic sizing (Monodisperse)	LDI	Linear then Reflectron Time-of-Flight	First to utilize dual polarity TOFMS and report + and - ion spectra for single particle.	194-196



utilizing 70 eV, may allow for the development of laser desorption/ionization libraries. Unfortunately, standards will be more difficult to come by than traditional EI due to differences in ionization from matrix effects, among other things, which must be studied in greater detail. If libraries are formed, they will not only help in the determination of species but also help in making this a more common technique.

Quantitation with LDI is another difficulty. It can be caused from particle-to-particle variability in ion signal due to particles undergoing LDI in hot spots within the laser beam (see Section II-C for other inherent laser problems). Johnston and Wexler along with other researchers have illustrated more complications. They have shown that a reproducible matrix and particle morphology is needed to quantify species. Relative humidity, ionization wavelength, along with variable laser powers all affect mass spectral signal intensities. To overcome these limitations, homogenizing the DI laser could be an important step because without knowing the exact power density applied and absorbed by the particle, quantitation is difficult. In addition, today's possible alternatives include averaging spectra during laboratory studies, therefore reducing the significance of shot-to-shot variations, and/or utilizing microdroplets, which allow for a more reproducible matrix and particle morphology than solid aerosols.

Other single particle techniques are beginning to arise because of this quantitation problem. Several groups have chosen to use surface vaporization coupled with EI ionization and a quadrupole mass spectrometer. This technique does have the ability to quantitate certain species within single particles. However, because of the scanning nature of the quadrupole, the entire mass spectrum cannot be obtained for each single particle.

This field, although in its early stages, is attempting to develop many different options to analyze aerosols. Depending on the specific application, off-line techniques can be used or on-line techniques can offer unique improvements that are instrument specific. For example, Murphy's instrument has been used for lower stratospheric particle measurements. Ramsey and Whitten's would be the current instrument of choice when analyzing complicated organic molecules from a specific source, as MS/MS can be utilized to aid in discerning chemical structures. Prather's field transportable instruments and their ability to obtain precise particle size and complete chemical composition have been shown to provide unique ambient data in a variety of locations. Reents or Ramsey and Whitten's, RSMS II, systems do not rely on optical detection and therefore can analyze particles less than 100 nm. Newer instruments such as Ziemann's and Jayne's are ideal for quantitating specific species within aerosols. It has been shown that each instrument, although put into an off-line or on-line classification and utilizing different ionization sources and mass spectrometers all have specific applications that have greatly added to this new and exciting field. In conclusion, aerosol mass spectrometry has proven to be an essential component in single particle analysis and will continue advancing

the aerosol field with its continued instrumentation improvements and countless laboratory and ambient applications.

## VI. Acknowledgments

The authors thank Dr. Chris Noble, Phil Silva, and Brad Morrical for their invaluable assistance during the reference acquisition period. We also thank Dr. Chris Noble, once again, and Dr. Toni Miguel for editing this article.

## VIII. References

- (1) Pope, C. A.; Dockery, W. D.; Spengler, J. D.; Raizenne, M. E. *Am. Rev. Respir. Dis.* **1991**, *144*, 668–674.
- (2) Dassen, W.; Brunekreef, B.; Hoek, G.; Hofschreuder, P.; Staatsen, B.; de Groot, H.; Schouten, E.; Biersteker, K. *J. Air Pollut. Control Assoc.* **1986**, *36*, 1223–1227.
- (3) Dockery, D. W.; Ware, J. H.; Ferris, B. G.; Speizer, F. E.; Cook, N. R.; Herman, S. M. *J. Air Pollut. Control Assoc.* **1982**, *32*, 937–942.
- (4) Dockery, D. W.; Speizer, F. E.; Stram, D. O.; Ware, J. H.; Spengler, J. D.; Ferris, B. G. *Am. Rev. Respir. Dis.* **1989**, *139*, 587–594.
- (5) Bates, D. V.; Sizto, R. *Environ. Res.* **1987**, *43*, 317–331.
- (6) Nevalainen, J.; Pekkanen, J. *Sci. Total Environ.* **1998**, *217*, 137–141.
- (7) Vedral, S. *J. Air Waste Manage. Assoc.* **1997**, *47*, 551–581.
- (8) Pope, C. A.; Thun, M. J.; Namboodiri, M. M.; Dockery, D. W.; Evans, J. S.; Speizer, F. E.; Heath, C. W. *Am. J. Respir. Crit. Care Med.* **1995**, *151*, 669–674.
- (9) Dockery, D. W.; Pope, C. A.; Xu, X.; Spengler, J. D.; Ware, J. H.; Fay, M. E.; Ferris, B. G.; Speizer, F. E. *N. Engl. J. Med.* **1993**, *329*, 1754–1759.
- (10) Wilson, W. E.; Suh, H. H. *J. Air Waste Manage. Assoc.* **1997**, *47*, 1238–1249.
- (11) Oberdorster, G.; Finkelstein, J.; Ferin, J.; Godleski, J.; Chang, L. Y.; Gelein, R.; Johnston, C.; Crapo, J. D. *Chest* **1996**, *109*, 68S–69S.
- (12) Phalen, R. F. *Toxicol. Lett.* **1998**, *96*, 263–267.
- (13) Raber, L. R. *Chem. Eng. News* **1997**, *4*, 110–18.
- (14) Kerr, R. A. *Sci.* **1997**, *276*, 1040–1042.
- (15) Mitchell, J. F. B.; Johns, T. C. *J. Clim.* **1997**, *10*, 245–267.
- (16) Dickinson, D. *Nat.* **1995**, *374*, 487.
- (17) Preining, O. *Sci. Total Environ.* **1992**, *126*, 199–204.
- (18) Erle, F.; Grendel, A.; Perner, D.; Platt, U.; Pfeilsticker, K. *Geophys. Res. Lett.* **1998**, *25*, 4329–4332.
- (19) Kotamarthi, V. R.; Rodriguez, J. M.; Sze, N. D.; Kondo, Y.; Pueschel, R.; Ferry, G.; Bradshaw, J.; Sandholm, S.; Gregory, G.; Davis, D.; Liu, S. *J. Geophys. Res.* **1997**, *102*, 28425–28436.
- (20) Tie, X.; Brasseur, G. *Geophys. Res. Lett.* **1996**, *23*, 2505–2508.
- (21) Lary, D. J.; Chipperfield, M. P.; Toumi, R.; Lenton, T. *J. Geophys. Res.* **1996**, *101*, 1489–1504.
- (22) Manion, J. A.; Fittschen, C. M.; Golden, D. M.; Williams, L. R.; Tolbert, M. A. *Isr. J. Chem.* **1994**, *34*, 355–363.
- (23) Considine, D. B.; Douglass, A. R.; Stolarski, R. S. *Geophys. Res. Lett.* **1992**, *19*, 397–400.
- (24) King, J. C.; Brune, W. H.; Toohey, D. W.; Rodriguez, J. M.; Starr, W. L.; Vedder, J. F. *Geophys. Res. Lett.* **1991**, *18*, 2273–2276.
- (25) Pitari, G.; Visconti, G.; Rizzi, V. *Geophys. Res. Lett.* **1991**, *18*, 833–836.
- (26) Rowland, F. S. *Annu. Rev. Phys. Chem.* **1991**, *42*, 731–768.
- (27) Molina, M. J. *Atmos. Environ.* **1991**, *25A*, 2535–2537.
- (28) Abbatt, J. P. D.; Molina, M. J. *Annu. Rev. Energy Environ.* **1993**, *18*, 1–29.
- (29) Peter, T. *Annu. Rev. Phys. Chem.* **1997**, *48*, 785–822.
- (30) Finlayson-Pitts, B. J.; Pitts, J. N. *Sci.* **1997**, *276*, 1045–1052.
- (31) Andreae, M. O.; Crutzen, P. J. *Sci.* **1997**, *276*, 1052–1058.
- (32) Ravishankara, A. R. *Sci.* **1997**, *276*, 1058–1065.
- (33) Hinds, W. C. *Aerosol Technology—Properties, Behavior, and Measurement of Airborne Particles*; John Wiley & Sons: New York, 1982.
- (34) Seinfeld, J. H.; Pandis, S. N. *Atmospheric Chemistry and Physics—From Air Pollution to Climate Change*; John Wiley & Sons: New York, 1998.
- (35) Kawamura, K. *Anal. Chem.* **1993**, *65*, 3505–3511.
- (36) Gundel, L. A.; Benner, W. H.; Hansen, A. D. A. *Atmos. Environ.* **1994**, *28*, 2715–2725.
- (37) Murphy, W. K.; Sears, G. W. *J. Appl. Phys.* **1964**, *35*, 1986.
- (38) Israel, G. W.; Friedlander, S. K. *J. Colloid Interface Sci.* **1967**, *24*, 330–337.
- (39) Dahneke, B. E.; Friedlander, S. K. *J. Aerosol Sci.* **1970**, *1*, 325–339.

- (40) Dahneke, B. In *Recent Developments in Aerosol Science*; Shaw, D. T., Ed.; John Wiley & Sons: New York, 1978.
- (41) Dahneke, B. E.; Cheng, Y. S. *J. Aerosol Sci.* **1979**, *10*, 257–274.
- (42) Cheng, Y. S.; Dahneke, B. E. *J. Aerosol Sci.* **1979**, *10*, 363–368.
- (43) Estes, T. J.; Vilker, V. L.; Friedlander, S. K. *J. Colloid Interface Sci.* **1983**, *93*, 84–94.
- (44) Liu, P.; Ziemann, P. J.; Kittelson, D. B.; McMurry, P. H. *Aerosol Sci. Technol.* **1995**, *22*, 293–313.
- (45) Liu, P.; Ziemann, P. J.; Kittelson, D. B.; McMurry, P. H. *Aerosol Sci. Technol.* **1995**, *22*, 314–324.
- (46) Skoog, D. A.; Leary, J. J. *Principles of Instrumental Analysis*, 4th ed.; Harcourt Brace College Publishers: San Diego, CA, 1992.
- (47) Benninghoven, A.; Rudenauer, F. G.; Werner, H. W. *Secondary Ion Mass Spectrometry*; Wiley: New York, 1987.
- (48) Christie, W. H. *Anal. Chem.* **1981**, *53*, 1240A–1242A.
- (49) Groenewold, G. S.; Delmore, J. E.; Olson, J. E.; Appelhans, A. D.; Ingram, J. C.; Dahl, D. A. *Int. J. Mass Spectrom. Ion Processes* **1997**, *163*, 185–195.
- (50) Wittmaack, K. *Int. J. Mass Spectrom. Ion Processes* **1995**, *143*, 19–27.
- (51) Davis, W. D. *Environ. Sci. Technol.* **1977**, *11*, 587–592.
- (52) Watson, J. T. *Introduction to Mass Spectrometry*, 3rd ed.; Lippincott-Raven: Philadelphia, PA, 1997.
- (53) Heinen, H. J. *Int. J. Mass Spectrom. Ion Phys.* **1981**, *38*, 309–322.
- (54) Van Der Peyl, G. J. Q.; Haverkamp, J.; Kistemaker, P. G. *Int. J. Mass Spectrom. Ion Phys.* **1982**, *42*, 125–141.
- (55) Cotter, R. J.; Tabet, J. C. *Int. J. Mass Spectrom. Ion Phys.* **1983**, *53*, 151–166.
- (56) Hercules, D. M.; Day, R. J.; Balasanmugam, K.; Dang, T. A.; Li, C. P. *Anal. Chem.* **1982**, *54*, 280A–305A.
- (57) Zhigilei, L. V.; Garrison, B. J. *Appl. Surf. Sci.* **1998**, *127–129*, 142–150.
- (58) Gross, D. S.; Gaelli, M. E.; Silva, P. S.; Prather, K. A. *Anal. Chem.* Submitted for publication.
- (59) Cotter, R. J. *Time-of-Flight Mass Spectrometry: Instrumentation and Applications in Biological Research*; ACS Professional Reference Books: Washington, DC, 1997.
- (60) Thomson, D. S.; Murphy, D. M. *Appl. Opt.* **1993**, *32*, 6818–6826.
- (61) Thomson, D. S.; Middlebrook, A. M.; Murphy, D. M. *Aerosol Sci. Technol.* **1997**, *26*, 544–559.
- (62) Simons, D. S. *Appl. Surf. Sci.* **1988**, *31*, 103–117.
- (63) Van Vaecck, L.; Struyf, H.; Van Roy, W.; Adams, F. *Mass Spectrom. Rev.* **1994**, *13*, 209–232.
- (64) Bruynseels, F. J.; Van Grieken, R. E. *Anal. Chem.* **1984**, *56*, 871–873.
- (65) Van Vaecck, L.; Bennett, J.; Van Epsen, P.; Schweikert, E.; Gijbels, R.; Adams, F.; Lauwers, W. *Org. Mass Spectrom.* **1989**, *24*, 782–796.
- (66) Van Vaecck, L.; Bennett, J.; Van Epsen, P.; Schweikert, E.; Gijbels, R.; Adams, F.; Lauwers, W. *Org. Mass Spectrom.* **1989**, *24*, 797–806.
- (67) Stoffels, J. J.; Ellis, D. R.; Bond, L. A.; Freedman, P. A.; Tattersall, B. N.; Lagergren, C. R. *Int. J. Mass Spectrom. Ion Processes* **1994**, *132*, 217–224.
- (68) Miller, P. E.; Denton, M. B. *J. Chem. Educ.* **1986**, *63*, 617–622.
- (69) Dawson, P. H. *Quadrupole Mass Spectrometry and Its Applications*; Elsevier: New York, 1976.
- (70) Cooks, R. G.; Glish, G. L.; McLuckey, S. A.; Kaiser, R. E. *Chem. Eng. News* **1991**, *3*, 26–41.
- (71) Yang, M.; Reilly, P. T. A.; Boraas, K. B.; Whitten, W. B.; Ramsey, J. M. *Rapid Commun. Mass Spectrom.* **1996**, *10*, 347–351.
- (72) Guan, S.; Marshall, A. G. *J. Am. Soc. Mass Spectrom.* **1994**, *5*, 64–71.
- (73) Eades, D. M.; Johnson, J. V.; Yost, R. A. *J. Am. Soc. Mass Spectrom.* **1993**, *4*, 917–929.
- (74) Weickhardt, C.; Moritz, F.; Grottemeyer, J. *Mass Spectrom. Rev.* **1996**, *15*, 139–162.
- (75) Gard, E.; Mayer, J. E.; Morrical, B. D.; Dienes, T.; Fergenson, D. P.; Prather, K. A. *Anal. Chem.* **1997**, *69*, 4083–4091.
- (76) Van Vaecck, L.; Struyf, H.; Van Roy, W.; Adams, F. *Mass Spectrom. Rev.* **1994**, *13*, 189–208.
- (77) Hercules, D. M.; Novak, F. P.; Viswanadham, S. K.; Wilk, Z. A. *Anal. Chim. Acta* **1987**, *195*, 61–71.
- (78) Denoyer, E.; Van Grieken, R.; Adams, F.; Natusch, D. F. S. *Anal. Chem.* **1982**, *54*, 26A–41A.
- (79) Wieser, P.; Wurster, R.; Haas, U. *Fresenius Z. Anal. Chem.* **1981**, *308*, 260–269.
- (80) Hachimi, A.; Van Vaecck, L.; Poels, K.; Adams, F.; Muller, J. F. *Spectrochim. Acta, Part B* **1998**, *53*, 347–365.
- (81) Bakker, A.; De Nollin, S.; Van Vaecck, L.; Slezak, J.; Ravingerova, T.; Jacob, W.; Ruigrok, T. J. C. *Life Sci.* **1995**, *56*, 1601–1611.
- (82) Mathey, A.; Van Vaecck, L.; Steglich, W. *Anal. Chim. Acta* **1987**, *195*, 89–96.
- (83) Colin, S.; Krier, G.; Jolibois, H.; Hachimi, A.; Muller, J. F.; Chambaudet, A. *Appl. Surf. Sci.* **1998**, *125*, 29–45.
- (84) Wonders, J. H. A. M.; Houweling, S.; DeBont, F. A. J.; Van Leeuwen, H. P.; Eeckhaudt, S. M.; Van Grieken, R. E. *Int. J. Environ. Anal. Chem.* **1994**, *56*, 193–205.
- (85) Struyf, H.; Van Vaecck, L.; Poels, K.; Van Grieken, R. *J. Am. Soc. Mass Spectrom.* **1998**, *9*, 482–497.
- (86) Poels, K.; Van Vaecck, L.; Gijbels, R. *Anal. Chem.* **1998**, *70*, 504–512.
- (87) Struyf, H.; Van Roy, W.; Van Vaecck, L.; Van Grieken, R.; Gijbels, R.; Caravatti, P. *Anal. Chim. Acta* **1993**, *283*, 139–151.
- (88) Fletcher, R. A. *Anal. Chem.* **1989**, *61*, 914–917.
- (89) Hara, K.; Kikuchi, T.; Furuya, K.; Hayashi, M.; Fujii, Y. *Environ. Sci. Technol.* **1996**, *30*, 385–391.
- (90) Dierck, I.; Michaud, D.; Wouters, L.; Van Grieken, R. *Environ. Sci. Technol.* **1992**, *26*, 802–808.
- (91) Wouters, L.; Artaxo, P.; Van Grieken, R. *Int. J. Environ. Anal. Chem.* **1990**, *38*, 427–438.
- (92) Van Borm, W.; Wouters, L.; Van Grieken, R.; Adams, F. *Sci. Total Environ.* **1990**, *90*, 55–66.
- (93) Mauney, T.; Adams, F. *Sci. Total Environ.* **1984**, *36*, 215–224.
- (94) Wouters, L.; Hagedoren, S.; Dierck, I.; Artaxo, P.; Van Grieken, R. *Atmos. Environ.* **1993**, *27A*, 661–668.
- (95) Otten, P.; Bruynseels, F.; Van Grieken, R. *Anal. Chim. Acta* **1987**, *195*, 117–124.
- (96) Bruynseels, F.; Storms, H.; Tavares, T.; Van Grieken, R. *Int. J. Environ. Anal. Chem.* **1985**, *23*, 1–14.
- (97) Tourmann, J. L.; Kaufmann, R. *Int. J. Environ. Anal. Chem.* **1993**, *52*, 215–227.
- (98) Jambers, W.; De Bock, L.; Van Grieken, R. *Analyst* **1995**, *120*, 681–692.
- (99) Lancin, M.; Le Strat, E.; Fries, E.; Miloche, M. *Int. J. Mass Spectrom. Ion Processes* **1997**, *163*, 69–79.
- (100) Groenewold, G. S.; Gianotto, A. K.; Olson, J. E.; Appelhans, A. D.; Ingram, J. C.; Delmore, J. E.; Shaw, A. D. *Int. J. Mass Spectrom. Ion Processes* **1998**, *174*, 129–142.
- (101) Bentz, J. W. G.; Goschnick, J.; Schuricht, J.; Ache, H. J.; Zehnpeffnig, J.; Benninghoven, A. *Fresenius J. Anal. Chem.* **1995**, *353*, 603–608.
- (102) Faude, F.; Goschnick, J. *Fresenius J. Anal. Chem.* **1997**, *358*, 67–72.
- (103) Fichtner, M.; Lipp, M.; Goschnick, J.; Ache, H. J. *Surf. Interface Anal.* **1991**, *17*, 151–157.
- (104) Goschnick, J.; Fichtner, M.; Lipp, M.; Schuricht, J.; Ache, H. J. *Appl. Surf. Sci.* **1993**, *70*, 63–67.
- (105) Berghmans, P.; Injuk, J.; Van Grieken, R.; Adams, F. *Anal. Chim. Acta* **1994**, *297*, 27–42.
- (106) Jalkanen, L. M.; Hasanen, E. K. *J. Anal. At. Spectrom.* **1996**, *11*, 365–369.
- (107) Nomizu, T.; Kaneco, S.; Tanaka, T.; Yamamoto, T.; Kawaguchi, H. *Anal. Sci.* **1993**, *9*, 843–846.
- (108) Kaneco, S.; Nomizu, T.; Tanaka, T.; Mizutani, N.; Kawaguchi, H. *Anal. Sci.* **1995**, *11*, 835–840.
- (109) Stoffels, J. J.; Allen, J. In *Physical and Chemical Characterization of Individual Airborne Particles*; Spurny, K. R., Ed.; John Wiley & Sons: New York, 1986.
- (110) Johnston, M. V.; Wexler, A. S. *Anal. Chem.* **1995**, *67*, 721A–726A.
- (111) Wood, S. H.; Prather, K. A. *Trends Anal. Chem.* **1998**, *17*, 346–356.
- (112) Davis, W. D. *J. Vac. Sci. Technol.* **1973**, *10*, 278.
- (113) Davis, W. D. *Environ. Sci. Technol.* **1977**, *11*, 593–596.
- (114) Lassiter, W. S.; Moen, A. L. *NASA Technical Memorandum X-3112* **1974**, 1–15.
- (115) Myers, R. L.; Fite, W. L. *Environ. Sci. Technol.* **1975**, *9*, 334–336.
- (116) Myers, R. L.; Fite, W. L. *Am. Lab.* **1975**, *7*, 23–29.
- (117) Stoffels, J. J.; Lagergren, C. R. *Int. J. Mass Spectrom. Ion Phys.* **1981**, *40*, 243–254.
- (118) Stoffels, J. J. *Int. J. Mass Spectrom. Ion Phys.* **1981**, *40*, 223–234.
- (119) Stoffels, J. J. *Int. J. Mass Spectrom. Ion Phys.* **1981**, *40*, 217–222.
- (120) Stoffels, J. J. *Int. J. Mass Spectrom. Ion Phys.* **1982**, *42*, 213–214.
- (121) Stoffels, J. J.; Laue, H. J. *Int. J. Mass Spectrom. Ion Processes* **1991**, *105*, 225–238.
- (122) Stoffels, J. J.; Laue, H. J. *Int. J. Mass Spectrom. Ion Processes* **1992**, *114*, 47–60.
- (123) Stoffels, J. J.; Wacker, J. F.; Kelley, J. M.; Bond, L. A.; Kiddy, R. A.; Brauer, F. P. *Appl. Spectrosc.* **1994**, *48*, 1326–1330.
- (124) Allen, J.; Gould, R. K. *Rev. Sci. Instrum.* **1981**, *52*, 804–809.
- (125) Sinha, M. P.; Giffin, C. E.; Norris, D. D.; Estes, T. J.; Vilker, V. L.; Friedlander, S. K. *J. Colloid Interface Sci.* **1982**, *87*, 140–153.
- (126) Sinha, M. P.; Friedlander, S. K. *Anal. Chem.* **1985**, *57*, 1880–1883.
- (127) Sinha, M. P.; Tomassian, A. D. *Rev. Sci. Instrum.* **1991**, *62*, 2618–2620.
- (128) Sinha, M. P. In *Particles in Gases and Liquids 2*; Mittal, K. I., Ed.; Plenum Press: New York, 1990.



- (129) Sinha, M. P.; Platz, R. M.; Vilker, V. L.; Friedlander, S. K. *Int. J. Mass Spectrom. Ion Processes* **1984**, *57*, 125–133.
- (130) Sinha, M. P.; Platz, R. M.; Friedlander, S. K.; Vilker, V. L. *Appl. Environ. Microbiol.* **1985**, *49*, 1366–1373.
- (131) Sinha, M. P.; Friedlander, S. K. *J. Colloid Interface Sci.* **1986**, *112*, 573–582.
- (132) Giggy, C. L.; Friedlander, S. K.; Sinha, M. P. *Atmos. Environ.* **1989**, *23*, 2223–2229.
- (133) Sinha, M. P. *Rev. Sci. Instrum.* **1984**, *55*, 886–891.
- (134) Sinha, M. P. *Appl. Spectrosc. Mater. Sci.* **1991**, *1437*, 150–156.
- (135) Marijnissen, J.; Scarlett, B.; Verheijen, P. *J. Aerosol Sci.* **1988**, *19*, 1307–1310.
- (136) McKeown, P. J.; Johnston, M. V.; Murphy, D. M. *Anal. Chem.* **1991**, *63*, 2069–2073.
- (137) Carson, P. G.; Neubauer, K. R.; Johnston, M. V.; Wexler, A. S. *J. Aerosol Sci.* **1995**, *26*, 535–545.
- (138) Mallina, R. V.; Johnston, M. V.; Wexler, A. S. *Abstracts of the Fourth International Aerosol Conference 1994*, 195–196 Los Angeles, CA.
- (139) Carson, P. G.; Johnston, M. V.; Wexler, A. S. *Rapid Commun. Mass Spectrom.* **1997**, *11*, 993–996.
- (140) Ge, Z.; Wexler, A. S.; Johnston, M. V. *Environ. Sci. Technol.* **1998**, *32*, 3218–3223.
- (141) Reents, W. D.; Downey, S. W.; Emerson, A. B.; Muijsce, A. M.; Muller, A. J.; Siconolfi, D. J.; Sinclair, J. D.; Swanson, A. G. *Plasma Sources Sci. Technol.* **1994**, *3*, 369–372.
- (142) Reents, W. D.; Downey, S. W.; Emerson, A. B.; Muijsce, A. M.; Muller, A. J.; Siconolfi, D. J.; Sinclair, J. D.; Swanson, A. G. *Aerosol Sci. Technol.* **1995**, *23*, 263–270.
- (143) Mallina, R. V. Ph.D. Dissertation, University of Delaware, 1998.
- (144) Mansoori, B. A.; Johnston, M. V.; Wexler, A. S. *Anal. Chem.* **1994**, *66*, 3681–3687.
- (145) Mansoori, B. A.; Johnston, M. V.; Wexler, A. S. *Anal. Chem.* **1996**, *68*, 3595–3601.
- (146) Neubauer, K. R.; Sum, S. T.; Johnston, M. V.; Wexler, A. S. *J. Geophys. Res.* **1996**, *101*, 18701–18707.
- (147) Neubauer, K. R.; Johnston, M. V.; Wexler, A. S. *Int. J. Mass Spectrom. Ion Processes* **1995**, *151*, 77–87.
- (148) Ge, Z.; Wexler, A. S.; Johnston, M. V. *J. Colloid Interface Sci.* **1996**, *183*, 68–77.
- (149) Carson, P. G.; Johnston, M. V.; Wexler, A. S. *Aerosol Sci. Technol.* **1997**, *26*, 291–300.
- (150) Neubauer, K. R.; Johnston, M. V.; Wexler, A. S. *Atmos. Environ.* **1998**, *32*, 2521–2529.
- (151) Ge, Z.; Wexler, A. S.; Johnston, M. V. *J. Phys. Chem. A* **1998**, *102*, 173–180.
- (152) Mallina, R. V.; Wexler, A. S.; Johnston, M. V. *J. Aerosol Sci.* **1997**, *28*, 223–238.
- (153) Thomson, D. S.; Murphy, D. M. *Chemtech* **1994**, *24*, 30–35.
- (154) Murphy, D. M.; Thomson, D. S. *Aerosol Sci. Technol.* **1995**, *22*, 237–249.
- (155) Murphy, D. M.; Thomson, D. S.; Middlebrook, A. M.; Schein, M. E. *J. Geophys. Res.* **1998**, *103*, 16485–16491.
- (156) Murphy, D. M.; Thomson, D. S.; Kaluzhny, M.; Marti, J. J.; Weber, R. J. *J. Geophys. Res.* **1997**, *102*, 6325–6330.
- (157) Murphy, D. M.; Thomson, D. S. *J. Geophys. Res.* **1997**, *102*, 6341–6352.
- (158) Murphy, D. M.; Thomson, D. S. *J. Geophys. Res.* **1997**, *102*, 6353–6368.
- (159) Murphy, D. M.; Thomson, D. S.; Middlebrook, A. M. *Geophys. Res. Lett.* **1997**, *24*, 3197–3200.
- (160) Middlebrook, A. M.; Murphy, D. M.; Thomson, D. S. *J. Geophys. Res.* **1998**, *103*, 16475–16483.
- (161) Murphy, D. M.; Anderson, J. R.; Quinn, P. K.; McInnes, L. M.; Brechtel, F. J.; Kreidenweis, S. M.; Middlebrook, A. M.; Posfai, M.; Thomson, D. S.; Buseck, P. R. *Nature* **1998**, *392*, 62–65.
- (162) Middlebrook, A. M.; Thomson, D. S.; Murphy, D. M. *Aerosol Sci. Technol.* **1997**, *27*, 293–307.
- (163) Murphy, D. M.; Thomson, D. S.; Mahoney, M. J. *Sci.* **1998**, *282*, 1664–1669.
- (164) Prather, K. A.; Nordmeyer, T.; Salt, K. *Anal. Chem.* **1994**, *66*, 1403–1407.
- (165) Nordmeyer, T.; Prather, K. A. *Anal. Chem.* **1994**, *66*, 3540–3542.
- (166) Noble, C. A.; Nordmeyer, T.; Salt, K.; Morrical, B.; Prather, K. A. *Trends Anal. Chem.* **1994**, *13*, 218–222.
- (167) Gaelli, M.; Guazzotti, S.; Prather, K. A. *Aerosol Sci. Technol.* Submitted for publication.
- (168) Salt, K.; Noble, C. A.; Prather, K. A. *Anal. Chem.* **1996**, *68*, 230–234.
- (169) Morrical, B. D.; Fergenson, D. P.; Prather, K. A. *J. Am. Soc. Mass Spectrom.* **1998**, *9*, 1068–1073.
- (170) Silva, P. J.; Prather, K. A. *Environ. Sci. Technol.* **1997**, *31*, 3074–3080.
- (171) Noble, C. A.; Prather, K. A. *Aerosol Sci. Technol.* **1998**, *29*, 294–306.
- (172) Noble, C. A.; Prather, K. A. *Appl. Occup. Environ. Hyg.* **1998**, *13*, 439–443.
- (173) Noble, C. A.; Prather, K. A. *Environ. Sci. Technol.* **1996**, *30*, 2667–2680.
- (174) Liu, D.; Rutherford, D.; Kinsey, M.; Prather, K. A. *Anal. Chem.* **1997**, *69*, 1808–1814.
- (175) Noble, C. A.; Prather, K. A. *Geophys. Res. Lett.* **1997**, *24*, 2753–2756.
- (176) Langer, S.; Pemberton, R. S.; Finlayson-Pitts, B. J. *J. Phys. Chem. A* **1997**, *101*, 1277–1286.
- (177) Vogt, R.; Crutzen, P. J.; Sander, R. *Nature* **1996**, *383*, 327–330.
- (178) Pszenny, A. A. P.; Keene, W. C.; Jacob, D. J.; Fan, S.; Maben, J. R.; Zetwo, M. P.; Springeryoung, M.; Galloway, J. N. *Geophys. Res. Lett.* **1993**, *20*, 699–702.
- (179) Gard, E. E.; Kleeman, M. J.; Gross, D. S.; Hughes, L. S.; Allen, J. O.; Morrical, B. D.; Fergenson, D. P.; Dienes, T.; Gaelli, M. E.; Johnson, R. J.; Cass, G. R.; Prather, K. A. *Science* **1998**, *279*, 1184–1187.
- (180) Dale, J. M.; Yang, M.; Whitten, W. B.; Ramsey, J. M. *Anal. Chem.* **1994**, *66*, 3431–3435.
- (181) Yang, M.; Dale, J. M.; Whitten, W. B.; Ramsey, J. M. *Anal. Chem.* **1995**, *67*, 4330–4334.
- (182) Yang, M.; Dale, J. M.; Whitten, W. B.; Ramsey, J. M. *Anal. Chem.* **1995**, *67*, 1021–1025.
- (183) Yang, M.; Whitten, W. B.; Ramsey, J. M. *Rev. Sci. Instrum.* **1995**, *66*, 5222–5225.
- (184) Reilly, P. T. A.; Gieray, R. A.; Yang, M.; Whitten, W. B.; Ramsey, J. M. *Anal. Chem.* **1997**, *69*, 36–39.
- (185) Gieray, R. A.; Reilly, P. T. A.; Yang, M.; Whitten, W. B.; Ramsey, J. M. *J. Microbiol. Methods* **1997**, *29*, 191–199.
- (186) Gieray, R. A.; Reilly, P. T. A.; Yang, M.; Whitten, W. B.; Ramsey, J. M. *Anal. Chem.* **1998**, *70*, 117–120.
- (187) Reilly, P. T. A.; Gieray, R. A.; Whitten, W. B.; Ramsey, J. M. *Environ. Sci. Technol.* **1998**, *32*, 2672–2679.
- (188) Murray, K. K.; Lewis, T. M.; Beeson, M. D.; Russell, D. H. *Anal. Chem.* **1994**, *66*, 1601–1609.
- (189) Murray, K. K.; Russell, D. H. *Anal. Chem.* **1993**, *65*, 2534–2537.
- (190) Fei, X.; Wei, G.; Murray, K. K. *Anal. Chem.* **1996**, *68*, 1143–1147.
- (191) Murray, K. K.; Russell, D. H. *J. Am. Soc. Mass Spectrom.* **1994**, *5*, 1–9.
- (192) Beeson, M. D.; Murray, K. K.; Russell, D. H. *Anal. Chem.* **1995**, *67*, 1981–1986.
- (193) Russell, D. H.; Beeson, M. D. *J. Mass Spectrom.* **1996**, *31*, 295–302.
- (194) Hinz, K. P.; Kaufmann, R.; Spengler, B. *Anal. Chem.* **1994**, *66*, 2071–2076.
- (195) Hinz, K. P.; Kaufmann, R.; Spengler, B. *Aerosol Sci. Technol.* **1996**, *24*, 233–242.
- (196) Kaufmann, R.; Chaurand, P.; Kirsch, D.; Spengler, B. *Rapid Commun. Mass Spectrom.* **1996**, *10*, 1199–1208.
- (197) Kievit, O.; Weiss, M.; Verheijen, P. J. T.; Marijnissen, J. C. M.; Scarlett, B. *Chem. Eng. Commun.* **1996**, *151*, 79–100.
- (198) Weiss, M.; Verheijen, P. J. T.; Marijnissen, J. C. M.; Scarlett, B. *J. Aerosol Sci.* **1997**, *28*, 159–171.
- (199) Alvarez, M. M.; Vezmer, I.; Whetten, R. L. *J. Aerosol Sci.* **1998**, *29*, 115–127.
- (200) Tobias, H. J.; Kooiman, P. M.; Docherty, K. S.; Ziemann, P. J. *Aerosol Sci. Technol.* Submitted for publication.
- (201) Jayne, J. T.; Leard, D. C.; Zhang, X.; Davidovits, P.; Smith, K. A.; Kolb, C. E.; Worsnop, D. R. *Aerosol Sci. Technol.* Submitted for publication.
- (202) Arnold, F.; Curtius, J.; Spreng, S.; Deshler, T. *J. Atmos. Chem.* **1998**, *30*, 3–10.
- (203) Schreiner, J.; Voigt, C.; Kohlmann, A.; Arnold, F.; Mauersberger, K.; Larsen, N. *Science* **1999**, *283*, 968–970.
- (204) Hoffmann, T.; Bandur, R.; Marggraf, U.; Linscheid, M. *J. Geophys. Res.* **1998**, *103*, 25569–25578.

CR9801380



